Electron Microscopy and Image Analysis of the Complexes I and V of the Mitochondrial Respiratory Chain

Brink, J.; Boekema, E.J.; Bruggen, E.F.J. van

Published in:
Electron Microscopy Reviews

DOI:
10.1016/0892-0354(88)90001-9

Publication date:
1988

Electron Microsc. Rev., Vol. 1, pp. 175–199, 1988
Printed in Great Britain.

0892-0354/88 $0.00 + 0.50

ELECTRON MICROSCOPY AND IMAGE ANALYSIS OF THE COMPLEXES I AND V OF THE MITOCHONDRIAL RESPIRATORY CHAIN

J. BRINK,* E. J. BOEKEMA† and E. F. J. VAN BRUGGEN*,‡

*Biochemisch Laboratorium, Rijksuniversiteit Groningen, Nijenborgh 16, NL-9747 AG Groningen, The Netherlands and
†Fritz-Haber-Institut der Max-Planck-Gesellschaft, Faradayweg 4–6, D-1000 Berlin, F.R.G.

CONTENTS

I. SCOPE OF THE REVIEW

The aim of this review is to summarize structural information on two membrane protein complexes of the eukaryotic respiratory chain. Special attention is paid to the elecron microscopy and subsequent image analysis. An extensive review on this subject has recently been published (Costello and Frey, 1987) dealing with the whole respiratory chain. This contribution, however, will focus on just two enzyme complexes, i.e. the NADH:ubiquinone oxidoreductase or NADH dehydrogenase (E.C. 1.6.99.3) and the F_0F_1 ATPase or ATP synthase (E.C. 3.6.1.3). This allows a more detailed discussion of many aspects not mentioned before. Moreover, new results have recently been achieved on both proteins. We will discuss structural aspects obtained by electron microscopy, and where possible functional aspects will be addressed and correlated with more general structural data. We assume that the reader is familiar with general principles of electron microscopy as well as image analysis. Therefore this review will not deal with

‡ To whom correspondence should be addressed.

the background of these techniques; instead, references to relevant papers will be provided.

II. MITOCHONDRIA

A. *Introduction*

In eukaryotic cells respiration is confined to a very specific particle, i.e. the mitochondrion. Mitochondria are highly specialized cell organelles, which supply metabolic energy in the form of ATP. In oxidative phosphorylation the ATP production is an exponent of actual cell respiration, which in itself is the result of the compartmentation of a specific set of enzymes, cofactors and substrates. Compartmentation is achieved by the presence of two continuous lipid bilayers, i.e. the inner membrane and the outer membrane. The outer membrane is permeable to small metabolites and ions, owing to the presence of a pore-forming protein, the mitochondrial porin (Mannella, 1982).

The inner membrane is extensively folded into a variable number of 'cristae mitochondriales' or cristae, which increase its total surface area. Together, the two bilayers enclose and define two mitochondrial compartments, i.e. the intercristae space or matrix space and the narrower intermembrane space. The latter is known to be connected to the intracristae space (Sjöstrand, 1983).

The matrix space contains several metabolic systems, such as the enzymes involved in the citric acid cycle and the β-oxidation of fatty acids. It also holds the enzymatic machinery responsible for the expression of the mitochondrial DNA (mtDNA). The mtDNA encodes only for a small fraction of the mitochondrial proteins, i.e. several polypeptides of NADH:ubiquinone (Q) oxidoreductase, cytochrome oxidase (complex IV) and ATP synthase (Tzagoloff, 1982; Tzagoloff and Myers, 1986). Seven unidentified reading frames of human mtDNA have been shown to encode for several subunits of the NADH:Q oxidoreductase (Chomyn *et al.*, 1985, 1986).

B. *The Respiratory Chain*

The citric acid cycle is responsible for the aerobic metabolism of acetyl-CoA and yields CO_2, metabolic intermediates and also NADH and $FADH_2$. The latter two are the substrates for the actual respiratory chain protein complexes. These proteins are located in the mitochondrial inner membrane. They catalyze a series of reactions, resulting in the transport of electrons from NADH and $FADH_2$ through the respiratory chain, after which the electrons are finally combined with molecular oxygen. The flow of these electrons liberates energy, which is conserved at three specific coupling sites numbered from 1 to 3. Numbers 1 to 3 refer to NADH:Q oxidoreductase, cytochrome reductase (complex III) and cytochrome oxidase, respectively. In the case of oxidative phosphorylation the ATP synthase (complex V), responsible for the ATP production, can be regarded as the fourth constituent of the respiratory chain.

The starting point in the respiratory chain is NADH:Q oxidoreductase, hereafter referred to as NADH dehydrogenase. This enzyme catalyzes the dehydrogenation of NADH by the removal of two electrons and two protons. These electrons and protons are transferred from riboflavin 5′-phosphate or flavine mononucleotide (FMN) via internal iron–sulphur (FeS) clusters to ubiquinone-10 (Q_{10} or coenzyme Q). The exact pathway of the protons is as yet not clear. The reduced ubiquinone, or ubiquinol, is oxidized in turn by cytochrome reductase, thereby regenerating the ubiquinone and restoring the pool-behaviour of ubiquinone with respect to NADH dehydrogenase and cytochrome reductase (Q-pool) (Slater, 1983; Ragan and Cottingham, 1985). Apparently NADH dehydrogenase combines with cytochrome reductase in a stoichiometric way to yield NADH-ferricytochrome *c* reductase activity, which accounts for the net flow of electrons towards cytochrome oxidase (Ragan and Heron, 1978). The dependence of this activity on the amount of exogenous lipid most likely implies a rate-limiting diffusion step as compared to the recombination and electron transfer rate of both enzymes (Schneider *et al.*, 1980). In line with the latter is the collision hypothesis (Herweijer *et al.*, 1985). The electrons are transferred via internal cytochromes *b* and c_1 and the Rieske FeS cluster (Rieske, 1976) to the one-electron acceptor ferri-

cytochrome *c*. Models describing the flow of electrons within the complexes III and IV have been presented in Wikström and Saraste (1984). The ferrocytochrome *c* is the substrate for the cytochrome oxidase, which transfers the electrons via cytochrome aa_3 to molecular oxygen.

During the transport of electrons through the respiratory chain, protons are translocated across the mitochondrial inner membrane at the coupling sites, resulting in an electrochemical potential ($\Delta\tilde{\mu}_{H^+}$). Possibly 12 protons are translocated for every oxygen atom reduced (Costello and Frey, 1987; Lane *et al.*, 1986). In the chemiosmotic hypothesis the $\Delta\tilde{\mu}_{H^+}$ is utilized by the ATP synthase to drive the phosphorylation of ADP to ATP using inorganic phosphate (Mitchell, 1961). A penetrating review on the chemiosmotic hypothesis appeared recently (Slater, 1987).

Detailed information regarding mitochondria and oxidative phosphorylation can be found in Lehninger (1964), Boyer *et al.* (1977), Tzagoloff (1982), Wikström and Saraste (1984) and Hatefi (1985a, b).

III. MITOCHONDRIAL NADH DEHYDROGENASE

A. *Introduction*

The mitochondrial NADH dehydrogenase catalyzes the first step in the respiratory chain. The enzyme is referred to as complex I or the particulate NADH dehydrogenase when isolated according to Hatefi *et al.* (1962). The enzyme oxidizes NADH coupled to the vectorial transport (translocation) of protons over the mitochondrial inner membrane. Despite intensive research for over more than two decades, the NADH dehydrogenase is still the least understood member of the respiratory chain proteins in terms of protein structure and mechanisms of electron transfer as well as proton translocation. Consequently, only deduced structural models exist. Reviews discussing the more general aspects of the respiratory chain protein complexes including NADH dehydrogenase can be found in Wikström and Saraste (1984) and Hatefi (1985a, b), whereas reference to NADH dehydrogenase in particular is made in Ragan (1976a, 1980, 1987).

B. *Subunits and Prosthetic Groups of NADH Dehydrogenase*

Most of the research has been devoted to the beef heart enzyme; other mammalian sources, however, have also been used, e.g. rabbit, rat and man (Cleeter and Ragan, 1985; Ragan, 1987). Furthermore, the enzyme from the fungus *Neurospora crassa* has also been studied (Ise *et al.*, 1985). The enzymes obtained from the various mammalian sources show immunological cross-reactivities (Cleeter and Ragan, 1985).

The NADH dehydrogenase contains FMN and FeS clusters. About 1.3 nmol FMN is present per mg protein (Ragan, 1976a) implying a minimal functional unit with a molecular mass of approximately 600–700 kDa (Ragan, 1980). Per FMN, roughly 17 to 23 gram atoms Fe are clustered with labile sulfide to several bi- and tetranuclear FeS clusters (Paech *et al.*, 1981; Ragan *et al.*, 1982a; Kowal *et al.*, 1986). The enzyme has been shown to contain four NADH-reducible FeS clusters (Beinert and Albracht, 1982; Kowal *et al.*, 1986), although a total number of up to eight to nine clusters has also been reported (Ohnishi *et al.*, 1985; Ragan, 1987). A tentative scheme for the spatial organization of these clusters has been presented (Ohnishi *et al.*, 1985). Detailed discussions concerning the FeS clusters can be found in Ohnishi (1979), Beinert and Albracht (1982) and Ohnishi and Salerno (1982).

The beef heart enzyme can be isolated in three distinct forms, all characterized by NADH-oxidation activity (Ragan, 1976b, 1980). The first two preparations refer to high molecular weight (type I) NADH dehydrogenases, i.e. the particulate NADH dehydrogenase and a water-soluble NADH dehydrogenase. Only the former has properties most closely resembling the coupling site 1 in mitochondria (Ragan, 1976a). In both preparations the enzyme contains up to 26 different polypeptides, as was shown using two-dimensional gel electrophoresis (Heron *et al.*, 1979).

The third enzyme preparation, called low molecular weight (type II) NADH dehydrogenase and

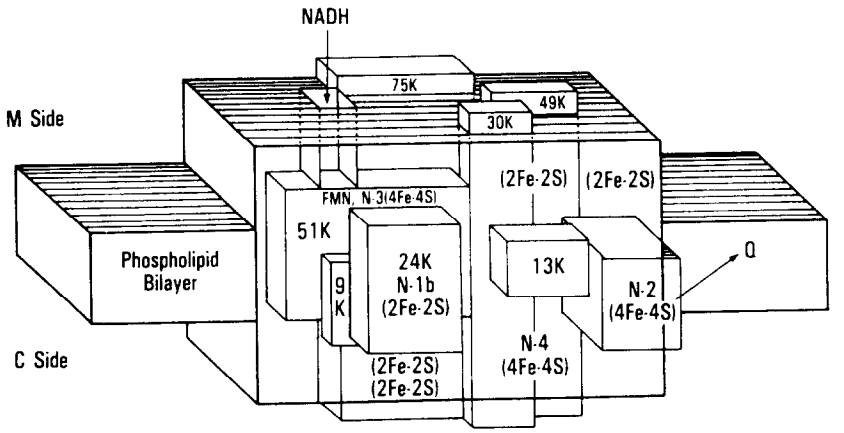

Fig. 1. Schematic representation of the arrangement of NADH dehydrogenase subunits and prosthetic groups in the mitochondrial inner membrane. The 9, 24, and 51 K blocks correspond to the FP subunits; the 13, 30, 49, and 75 K blocks are the FeS protein fragment subunits. The large block containing the FP and the FeS protein fragment is the insoluble residue. The approximate positions of the FeS clusters and the FMN are indicated. The relative size and placement of the protein blocks are not precise. Reproduced with permision of Plenum Press. Courtesy of Dr Y. Hatefi.

also a water-soluble form, was shown to be a fragment of the type I NADH dehydrogenase (Biggs *et al.*, 1963; Watari *et al.*, 1963). This preparation contains only three polypeptides with molecular masses of 9, 24 and 51 kDa (Ragan *et al.*, 1982a). Treatment of complex I with a NAD^+ derivative, i.e. arylazido-β-alanyl-NAD^+, indicated that the 51 kDa subunit comprises the NADH binding site (Chen and Guillory, 1981).

Upon chaotropic resolution the type I NADH dehydrogenase resolves into a water-soluble fraction and a water-insoluble fraction (Hatefi and Stempel, 1969; Ragan *et al.*, 1982a, b). The former can be further separated into an iron-enriched, but FMN-depleted fraction (the iron–sulphur protein fragment or FeS protein fragment) and an FMN-containing fraction (the flavoprotein fragment or the FP fragment). The FP fragment is identical to the type II NADH dehydrogenase. This fragment shows NADH-ubiquinone reductase activity and contains FMN as well as two FeS clusters (Ragan *et al.*, 1982b). The FeS cluster most probably involved in the interaction with FMN is cluster 3.

The second fraction, i.e. the FeS protein fragment, is composed of six subunits with molecular masses ranging from 13 to 75 kDa with a total molecular mass of 165 kDa. It contains nearly one half of the total Fe and exhibits no detectable oxidoreductase activity (Ragan *et al.*, 1982b).

The insoluble residue contains approximately 15 polypeptides all of extremely hydrophobic nature. Furthermore, two additional FeS clusters are present, which are not detected by means of electron paramagnetic resonance experiments on complex I, viz. EPR-silent in complex I (Hatefi *et al.*, 1985a).

C. *Chemical Labelling of NADH Dehydrogenase*

The hydrophilic nature of the FeS protein and FP fragments appears to contradict the lipophilic nature of the NADH dehydrogenase. Based upon chemical labelling studies with hydrophilic reagents, such as diazobenzenesulphonate and lactoperoxidase-catalyzed radioiodination, and hydrophobic probes such as 5-iodonaphth-1-yl azide and arylazidophosphatidylcholine, Ragan and coworkers have proposed a model which accounts for this apparent contradiction (Fig. 1). In this model both the FeS protein fragment and the FP fragment are surrounded by the hydrophobic subunits. The FP fragment is completely buried within the enzyme structure and thus shielded from the aqueous environment (Ragan, 1980; Ohnishi *et al.*,

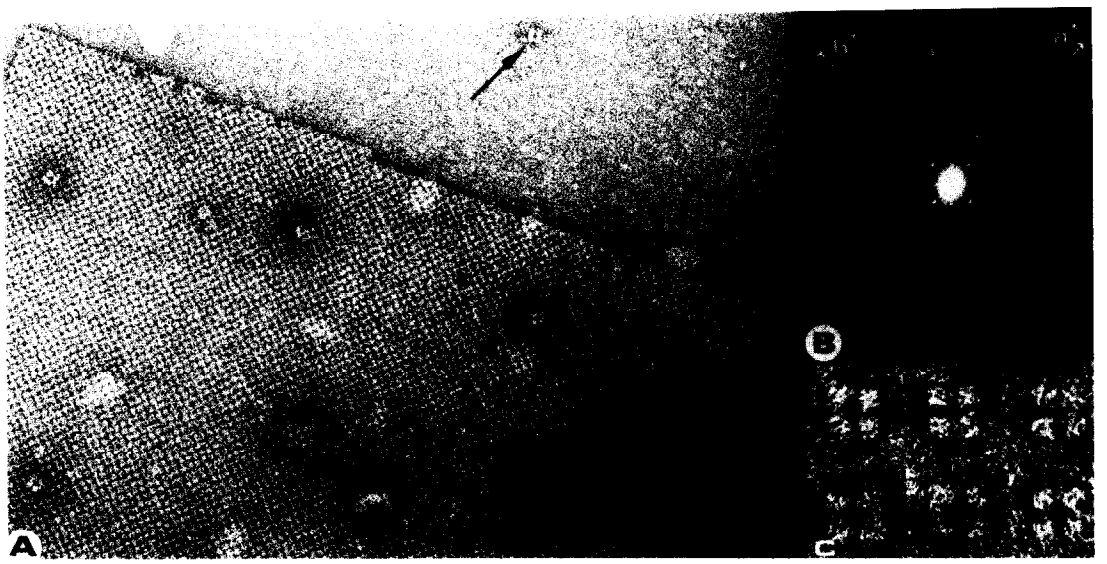

Fig. 2. Electron microscopy of beef heart NADH dehydrogenase. (A) Part of large monolayered crystal negatively stained with 1% uranyl acetate. Arrow indicates crystal's 'building block'. Scale marker represents 100 nm. (B) Optical diffraction pattern of such a crystal with indicated lattice vectors. Arrows indicate (7, 7) reflections equivalent to $1/1.5\,nm^{-1}$. (C) Selected views of crystal's 'building blocks'. Magnification is 500,000×. Reproduced with permission of Springer-Verlag.

1985; Ragan and Hatefi, 1986). Access of the NADH to the FP fragment in this model can be provided by means of a channel. This channel may be realized by the 49 and 75 kDa subunits of the FeS protein fragment (Chen and Guillory, 1981). Partial confirmation has been obtained from studies involving cleavable cross-linkers (Cleeter *et al.*, 1985; Gondal and Anderson, 1985).

D. *Electron Microscopy*

In contrast to many other types of research a relatively small number of electron microscopical studies concerning the structure of NADH dehydrogenase have been conducted. A few of the earliest electron micrographs of complex I-containing fractions were presented in Crane *et al.* (1969). They reported sheet-like structures approximately 7 nm thick, presumably of a membranous nature, in thin sections of mitochondrial subfractions. In negatively stained specimens membrane-associated globules with diameters of 4 to 5 nm were observed. Ragan and Racker (1973) also demonstrated the presence of membrane-associated globules in negatively stained specimens of complex I/phospholipid mixtures. Occasionally particles protruding some 8.5 nm from the membrane could be seen. Dialysis in the absence of phospholipids resulted in aggregates resembling those observed earlier by Crane. More detailed studies, however, emerged only recently by Boekema *et al.* (1982, 1984) and Brink *et al.* (1987) on the beef heart enzyme, and by Leonard *et al.* (1987) on the enzyme from *N. crassa*.

E. *Structure of Beef Heart NADH Dehydrogenase*

Boekema *et al.* (1982, 1986a) have demonstrated the possibility of obtaining large, well-ordered, rectangular two-dimensional crystals from complex I preparations after dialysis against 1.5 M of ammonium sulphate at slightly acidic pH (Fig. 2A). Several of the individual building blocks of these crystals are shown in Fig. 2C. These molecules are roughly 15 × 15 nm and have a tetragonal appearance. This has subsequently been confirmed by image analysis involving single-particle averaging, but details beyond 3 to 4 nm resolution were not retrieved (Boekema *et al.*, 1984). The two-

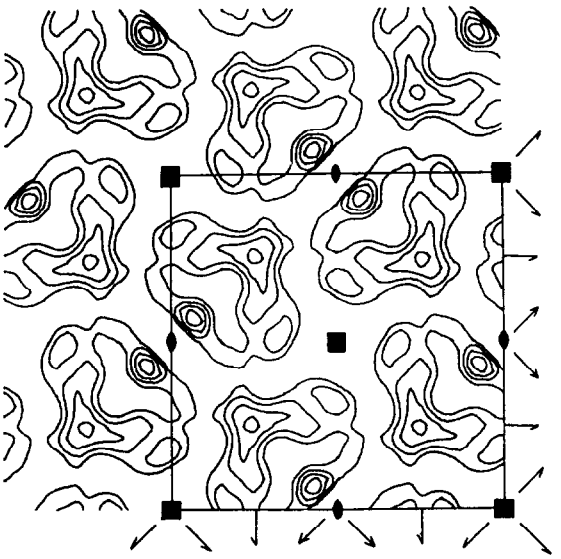

Fig. 3. Reconstructed projected structure of a crystal of beef heart NADH dehydrogenase. Contour plot with imposed $p42_12$ symmetry showing only positive contour levels. Unit cell and symmetry elements have been drawn; filled squares represent the four-fold rotation axes normal to the plane of the crystal. Unit cell dimensions are 15.3×15.3 nm. For details see Brink *et al.* (1987). Reproduced with permission of Springer-Verlag.

dimensional crystals, however, are most suitable for obtaining high-resolution data, since they are monolayered over considerable large areas. Their dimensions vary from 0.5 to 2.0 μm depending on the presence of NADH and dithiothreitol (Brink *et al.*, 1987). A typical optical diffraction pattern of these crystals after negative staining is shown in Fig. 2B. It displays *4mm*-symmetry, as can be judged from the apparent four-fold rotational symmetry relating all reflections with each other, and the mirror symmetry along lines running at 45° angles with the lattice vectors a and b. The lattice parameters were determined as $a = b = 15.3$ nm with $\gamma = 90°$.

Application of correlation averaging (Frank, 1982; Saxton and Baumeister, 1982) and subsequent real-space reconstruction of tilted views of these crystals yielded a three-dimensional structure with approximately 1.8 nm resolution (Boekema *et al.*, 1986a). Contrary to the first interpretation of this structure, viz. a dimer of NADH dehydrogenase molecules, Brink *et al.* (1987) showed that the crystals actually contained fragments of the enzyme. They identified the crystal symmetry as $p42_12$ by using a numerical analysis of the amplitudes and phases of all reflections. A contour plot showing the unit cell with imposed $p42_12$ symmetry as well as all symmetry elements is presented in Fig. 3. In parallel, half-tone images of the unit cell with similar orientations are shown in Fig. 4A and B. The unit cell is composed of four identical motifs, grouped around each four-fold rotational axis in the crystal. These motifs resemble a more or less distorted triangle with one central dark region. From crystallographic rules it was concluded that the unit cell contained 8 identical asymmetrical units, inferring that each motif should be equivalent to a dimer. The dark region in each motif corresponds to a pore extending through the entire structure, i.e. along the vertical c-axis, as was shown by Boekema *et al.* (1984, 1986a). Although Boekema's model exhibiting p2 symmetry was improved by Brink *et al.* (1987) by imposing the higher $p42_12$ symmetry, no additional information concerning the structure became available. Apparently each motif is a dimeric, ellipsoidal particle containing one pore.

In section IIIC the issue was raised concerning the constituents of the aqueous channel, by which access of NADH to the FP fragment is provided. It was established that both the 49 and 75 kDa subunits of the FeS protein fragment were involved (Cleeter *et al.*, 1985; Gondal and Anderson, 1985). Image analysis carried out by Brink *et al.* (1987) on the two-dimensional crystals after labelling with anti-(75 kDa subunit) F_{ab} indicated that the F_{ab} bound near the pores of the crystal (Fig. 5). Therefore the antigen, i.e. the 75 kDa subunit, is situated close to these pores. Similar immunolabelling experiments with anti-(49 kDa subunit) F_{ab} have shown that the crystals tend to dissociate during labelling (Brink and van Bruggen, unpublished results). No precise localization of the latter subunit was therefore possible, let alone a possible involvement in the realization of the pore.

Brink *et al.* (1987) postulated a hypothesis concerning the composition of the crystals. The authors suggested that the crystals were built of FeS protein fragments, which aggregate first up to a level of octamers, and second so as to yield the

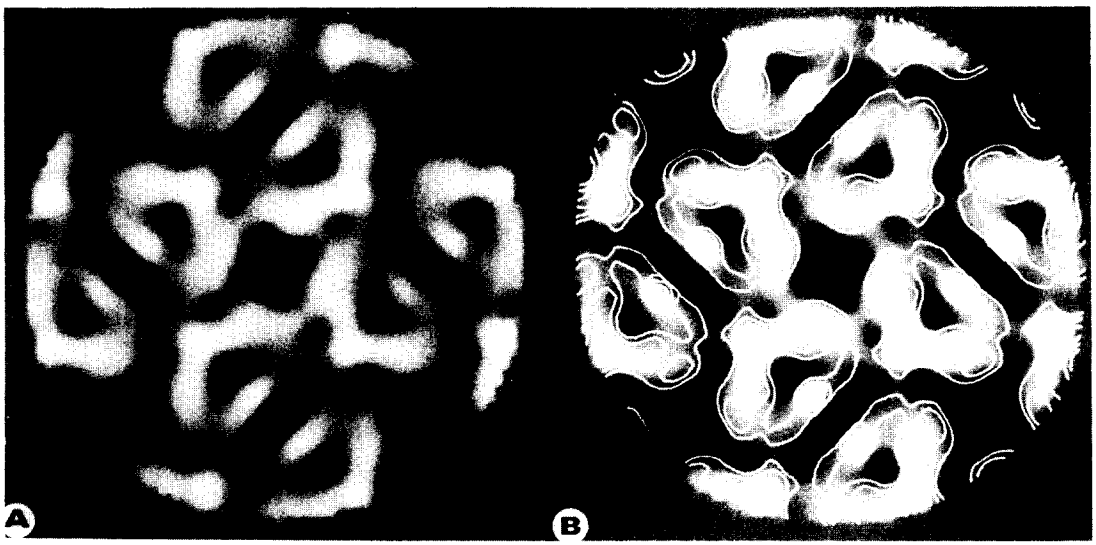

Fig. 4. Reconstructed projected structure of a crystal of beef heart NADH dehydrogenase. (A) Half-tone image in similar orientation as compared to Fig. 3. The four identical motifs arranged around the four-fold rotation axis in the centre of the unit cell are shown. Protein in the figure and hereafter appears white. (B) As in A, but the contour levels of Fig. 3 have been superimposed to facilitate correlation of Fig. 3 with the grey-scale image of A. Both half-tone images display p2 symmetry, except the contour levels, which display $p42_12$ symmetry. Scale marker represents 5 nm. Reproduced with permission of Elsevier Science Publishers B. V. Modified from Boekema *et al.* (1984).

two-dimensional crystals. They furthermore suggested that the crystallizing entity was identical to a dimeric particle. This dimer could be identical to some sort of core particle of a native dimeric NADH dehydrogenase complex (Dooijewaard and Slater, 1976a, b; Dooijewaard *et al.*, 1978; Albracht and Bakker, 1986; Bakker and Albracht, 1986). Both the FP fragments and the hydrophobic subunits could have been removed by mere fragmentation of the enzyme (Cremona *et al.*, 1963; Watari *et al.*, 1963; Rossi *et al.*, 1965) or by a preferential self-association of the removed subunits caused by ammonium sulphate, leaving as remainder the dimeric core particle, which subsequently aggregates. In such a particle the pore could then easily be part of the channel necessary for the NADH. The pore width of 2 nm might allow the NADH to reach the NADH binding site on the 51 kDa subunit of the FP fragment. Thus the close proximity of the 75 kDa subunit to the channel in the enzyme, and the localization of this subunit near the pores in the crystals, suggest a partial similarity between the channel and the pore. Nevertheless, since the precise relationship between the fragments in the crystal and the enzyme in the mitochondrial inner membrane is unknown, a firm statement concerning the physiological role of the pores cannot be made.

Besides the well-ordered, rectangular two-dimensional crystals, a second crystal form was observed under slightly altered conditions (Boekema and van Bruggen, 1983). Figure 6 shows a gallery of several patches of this crystal form. All exhibit a typical banded appearance caused by alternating light and dark rows of stain-excluding moieties. Lattice vector a was chosen parallel to the light rows with b approximately normal to a. Occasionally a striation can be observed running at 45° angles relative to a and b. This striation divides the large stain-excluding moieties in the unit cell into two equally large parts, thus creating the impression of two domains or two monomers within the unit cell. The crystalline nature of these patches is enhanced by the repeat distance (b) discernible in each row. The lattice parameters were determined as $a = 19 \pm 1.3$ nm, $b = 34 \pm 6$ nm with γ varying between 80° and 90°. Given the height of the enzyme of 8.5 nm (Ragan and Racker, 1973) a

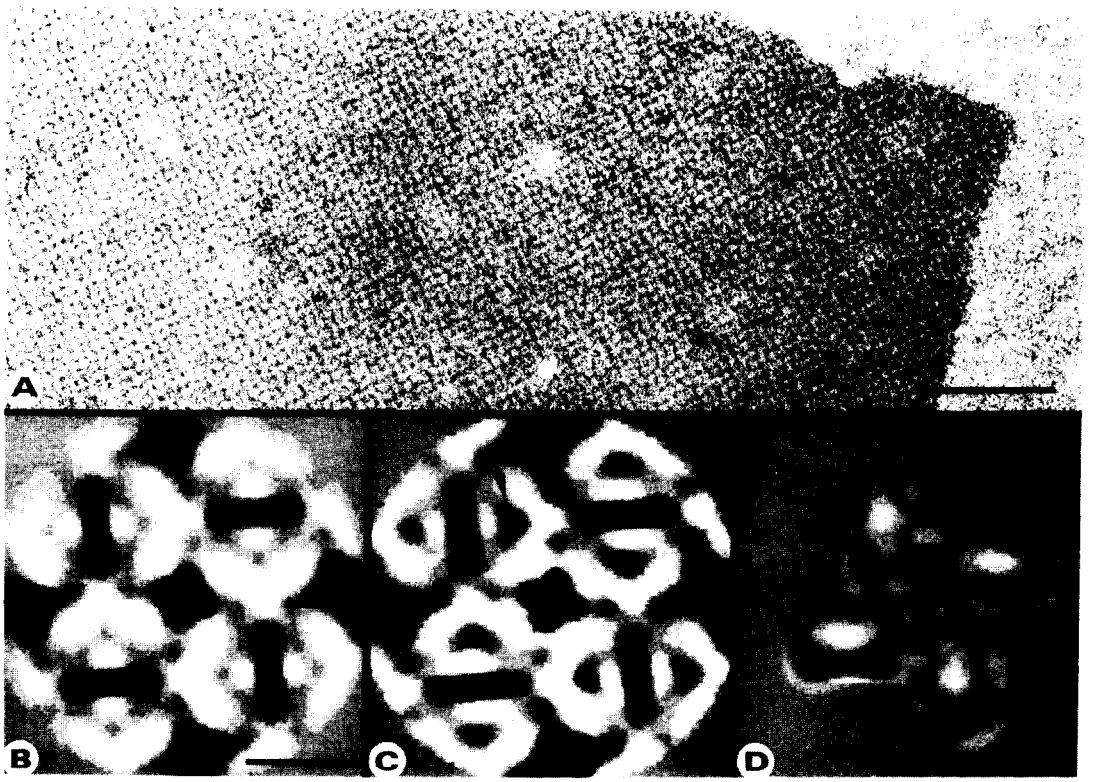

Fig. 5. Image analysis of two-dimensional crystals of beef heart NADH dehydrogenase after F_{ab} labelling. (A) Crystal after labelling with anti-(75 kDa subunit) F_{ab}; scale marker represents 100 nm. (B) Average of 4500 labelled motifs; scale marker represents 5 nm. (C) Similar to B, but 4300 untreated motifs averaged; arrow indicates one of the four large pores. (D) Fourier difference of B and C; white regions correspond to extra stain-exclusion in B. For details see Brink *et al.* (1987). Reproduced with permission of Springer-Verlag.

total unit cell volume of 8721 nm^3 is available. The unit cell is filled with stain-excluding moieties to an approximate level of only 50%. This can be judged from the large change in contrast in the unit cell, which corresponds to large differences in mass thickness. At an average molecular volume of 2.0×10^{-3} Da/nm^3 (Matthews, 1968), the total molecular mass in the unit cell would then be 2.2×10^6 Da. With a monomeric molecular mass of 600–700 kDa and allowing additional phospholipid and residual detergent to be present, this figure would then hint at two enzyme molecules occupying the unit cell. The aggregation state of the enzyme in the mitochondrial inner membrane, however, does not necessarily have to be similar to such a dimeric moiety. Indeed, this issue is a matter of dispute, as can be judged from the literature.

Since large monolayered crystals of the second form are unavailable a detailed description of the molecular packing is impossible. Nevertheless, some deductions can be made. Incorporation of the NADH dehydrogenase into lipid vesicles and subsequent detergent removal by dialysis failed to produce crystals (Brink and van Bruggen, unpublished results). Yet, from electron micrographs (Fig.7) an average height for the enzyme of 10 nm can be measured. Furthermore, from these side-on views a minimum repeat distance of 30 to 40 nm (roughly equal to b) can be measured. A smaller repeat distance has only occasionally been noticed. The similarity of the measured repeat distance with the lattice vector b suggests a molecular packing almost as in a two-dimensional crystal. This furthermore indicates that the vesicles have collapsed

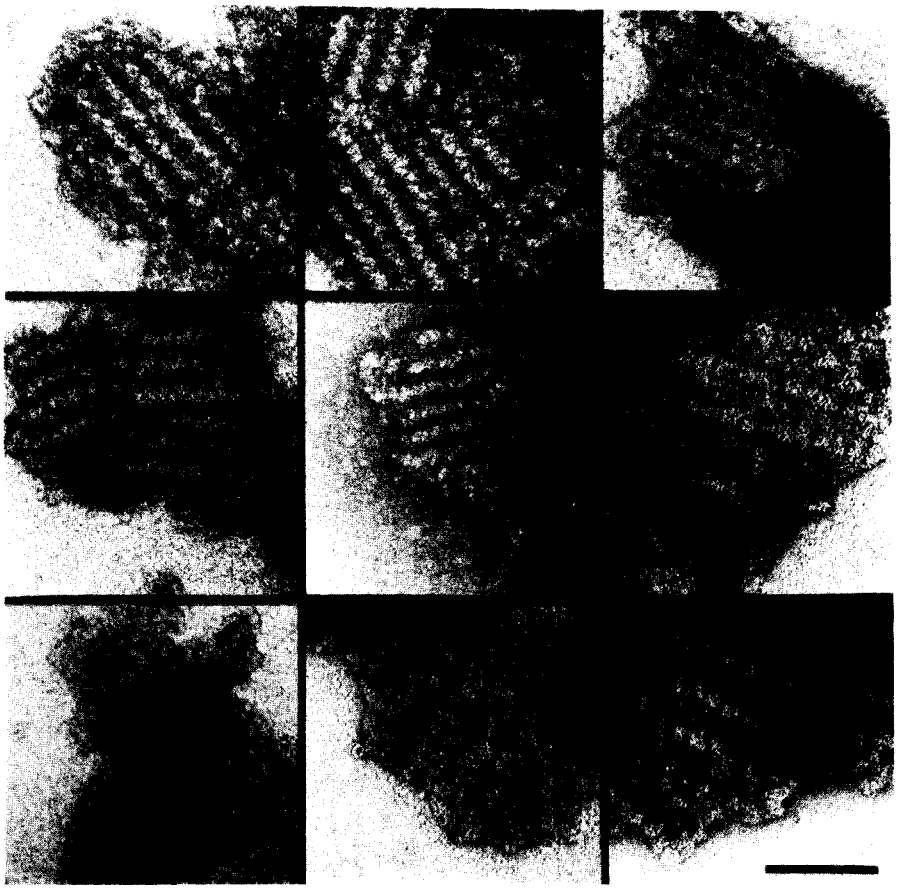

Fig. 6. Crystalline patches of native beef heart NADH dehydrogenase obtained after microdialysis at pH 7.0. The three left-hand side patches as well as the central one show clear striations running at approximately 45° angles relative to the vectors *a* and *b*. Scale marker represents 100 nm. For details see text.

so as to reveal mostly the largest repeat distance. Thus the side-on view of the molecules represents a view along the analogue of *a*. Above we showed the possible existence of a dimeric enzyme complex within the unit cell. Assuming individual enzyme molecules protruding from the membrane and a view along *a*, then only one of the two monomers is visible. Thus, the other monomer would face the vesicle's interior, viz. the monomers in the dimeric enzyme structure would be related by a two-fold rotation axis in the plane of the membrane. In a minimal enzyme configuration two clusters 2 are present for only one cluster 1, whereas cluster 2 occurs in a ratio of roughly 0.8:1 as compared to FMN (Beinert and Albracht, 1982). This could indicate that not only a structural difference between both protomers exists but also a functional one. Kinetic studies, however, may suggest no functional differences, since two competing NADH binding sites have been found either per FMN or per dimeric enzyme complex (Dooijewaard and Slater, 1976). The dimeric arrangement as outlined above, however, could imply that only one monomer participates in the vectorial transport of protons. Given the implication of this speculation more structural data on the enzyme in either two-dimensional crystals or the mitochondrial inner membrane are needed to substantiate a statement about the functional organization of NADH dehydrogenase.

Fig. 7. Gallery of side on views of beef heart NADH dehydrogenase after reincorporation into soyabean lecithin vesicles following the procedure of Hovmöller *et al.* (1983). Individual enzyme molecules have been indicated protruding approximately 10 nm from the membrane. Repeat distance is about 30 to 40 nm. Scale marker represents 100 nm.

F. *Structure of Fungal NADH Dehydrogenase*

Leonard *et al.* (1987) recently reported on the successful crystallization of mitochondrial NADH dehydrogenase from the fungus *N. crassa*. As was shown by Ise *et al.* (1985) this enzyme comprises more than 15 different polypeptides, with molecular masses ranging from 11 to 70 kDa and a total molecular mass of approximately 550 kDa. Similar to the beef heart enzyme, at least six subunits are coded by the mtDNA. No immunological relationship has been demonstrated for the fungal and beef heart enzyme. Isolation was accomplished by chromatographic procedures rather than differential ammonium sulphate precipitation as for bovine complex I (Hatefi *et al.*, 1962).

Crystallization was achieved by incorporation of the enzyme in phospholipid vesicles with subsequent detergent removal in a similar way as for cytochrome reductase (Hovmöller *et al.*, 1983). Crystals were obtained as double-layered vesicles or tubes (Fig. 8A) and as monolayered sheets (Fig. 8B). The former show a Moiré pattern arising from two overlapping crystalline layers. At the edges of these vesicle crystals single molecules can be seen protruding 10 nm from the membrane at regular intervals of about 31 nm.

The monolayered sheets are characterized by a banded appearance, similar to the small beef heart crystals seen in Fig. 6. The sheets appear to result from a side-long alignment of rows of one-dimensionally crystallized NADH dehydrogenase molecules. However, several regions with randomly oriented monomeric and occasionally dimeric enzyme complexes can be discerned. The crystalline regions have lattice parameters $a = 19$ nm, $b = 38$ nm and $\gamma = 90°$.

From the single-layered sheets a three-dimensional (3D) model was calculated using a Fourier synthesis to combine the Fourier data of several projections obtained at different tilt angles (Amos *et al.*, 1982). The contour plots (Fig. 9) show firm contacts between the molecules within each row, but barely discernible connections between the individual rows. Leonard *et al.* (1987) have calculated a stain-excluding volume associated with the protein of 2.5×10^3 nm^3, correspond-

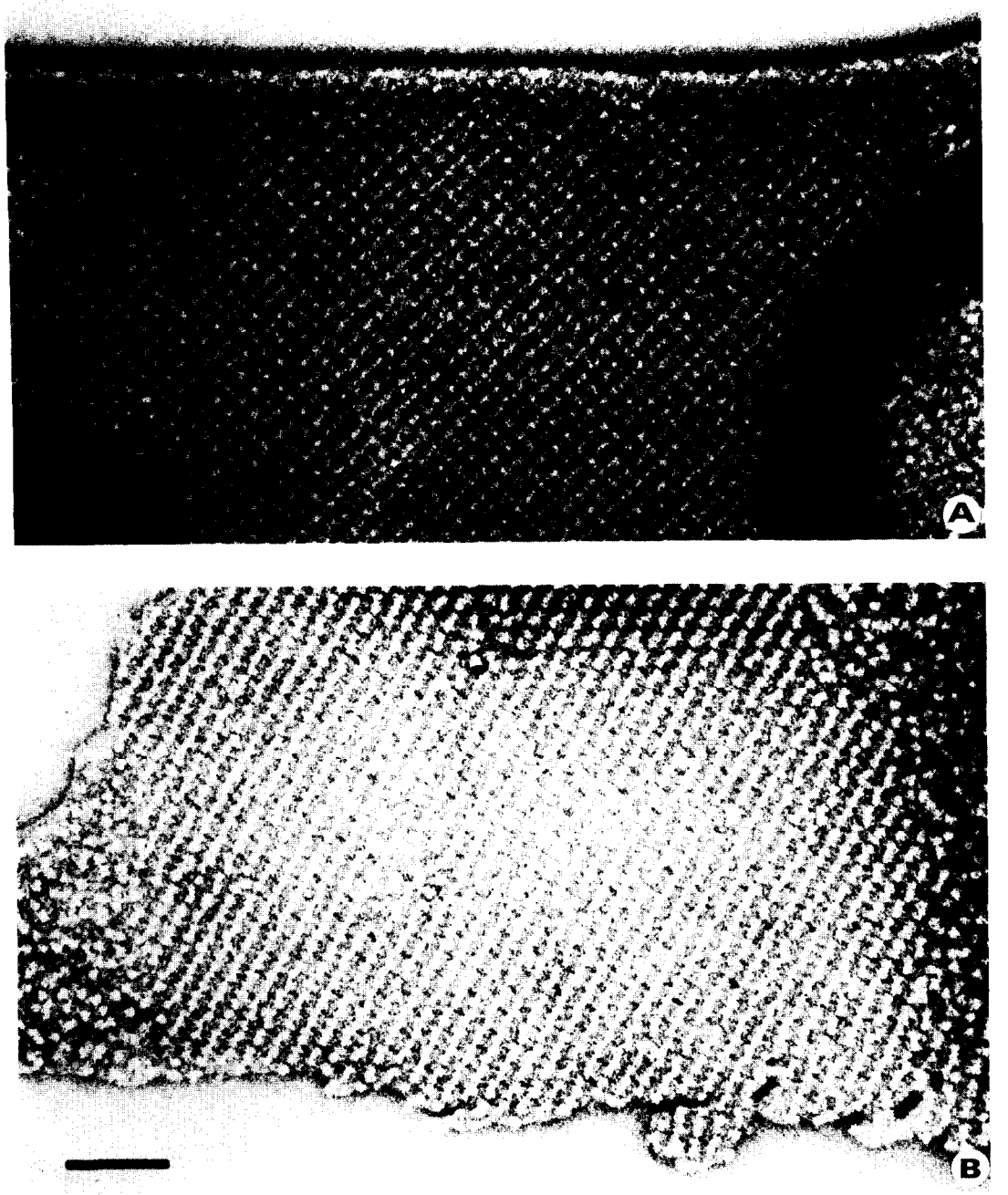

Fig. 8. Membrane crystals of fungal NADH dehydrogenase. (A) Double-layer membrane crystal. At the top edge where the crystal folds over, molecules can be seen on cross-section projecting about 10 nm from the surface. (B) Single-layer membrane crystal showing a large, well-ordered domain, with rows of molecules separated by about 20 nm. At the left and the right in B regions without crystallinity can be seen. Scale marker represents 100 nm. Reproduced with permission of Academic Press Inc. Courtesy of Dr K. Leonard.

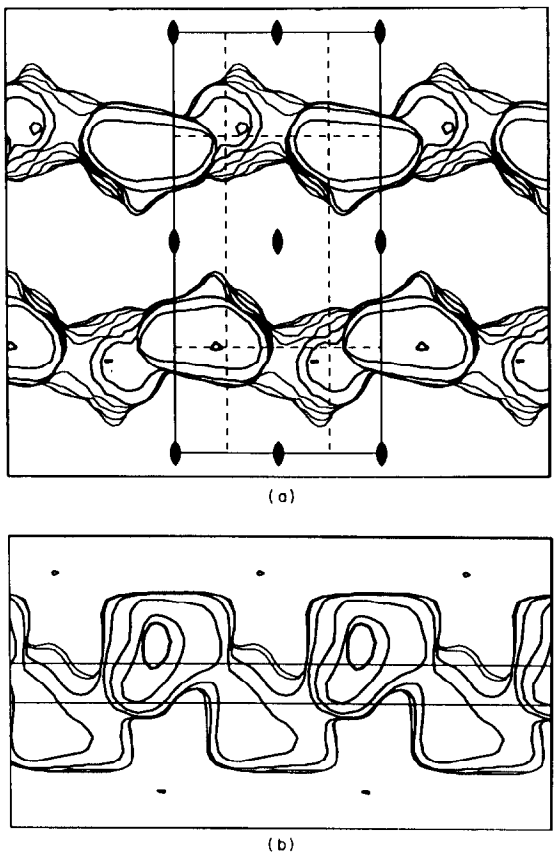

Fig. 9. Contour plots of fungal NADH dehydrogenase. (a) A hidden line plot of the three-dimensional reconstruction viewed normal to the plane of the membrane. (b) As (a), but now viewed in the plane of the membrane along *b*. Central parallel lines indicate the approximate position of the lipid bilayer. Large density domains can be seen projecting alternately above and below the membrane. For details see Leonard *et al.* (1987). Reproduced with permission of Academic Press Inc. Courtesy of Dr K. Leonard.

ing to a molecular mass of 2.0×10^6 Da at a protein density of 1.25 g/cm^3. Since the model clearly reveals four enzyme complexes, the non-proteinous volume will be occupied by a single lipid bilayer. The bilayer occupies about 400 nm^2, whereas the four enzyme complexes account for only 320 nm^2. This large amount of lipid is exclusively located between the stain-excluding rows of the enzyme complexes. This molecular packing is in striking contrast to the packing in two-dimensional crystals of cytochrome reductase (Leonard *et al.*, 1981), cytochrome oxidase (Deatherage *et al.*, 1982; Kim *et al.*, 1985) and, for instance, bacteriorhodopsin (Henderson *et al.*, 1986). In these crystals no direct contacts between the protein molecules exist, implying that all interactions are mediated through the lipid bilayer and therefore of hydrophobic nature. The interactions in the NADH dehydrogenase crystals will most probably occur via the protein parts (hydrophilic) as well as the bilayer parts (hydrophobic). This might explain the poor quality of the lattice, as reflected by the smeared-out reflections in the optical transform and the rather low resolution (Michel, 1983).

In the 3D model (Fig. 10) the molecules are placed asymmetrically with respect to the membrane, spanning a distance of about 15 nm. The enzyme protrudes some 9 to 10 nm from one side of the membrane, as was also observed in the side-on views of the vesicle crystals of the fungal enzyme, as well as previously with the beef heart enzyme. The small protrusion of 1 nm on the opposite side of the membrane seems questionable in view of the 3.9 nm resolution along *c*. Unfortunately, no information with respect to the orientation of the enzyme within the mitochondrial inner membrane was obtained. Leonard *et al.* (1987) questioned the labelling results obtained with hydrophilic probes. Failure to label the FP fragment with labels other than a NAD^+ analogue could arise from the compactness of the structure or from a shielding by peripherally located subunits. This argues against the existence of a well-defined channel for NADH. Labelling of the 49 and 75 kDa subunits would then have to be explained in terms of a specific binding or a recognition site for NADH on these subunits.

G. *Evaluation of State-of-the-art*

With the recent crystallization of the mitochondrial NADH dehydrogenase, the conclusion is that the overall structure for all enzyme complexes of the respiratory chain is known. The fact that from the beef heart enzyme, crystals were also obtained, although not yet optimal for image analysis, raises the question to what level both structures are similar. From the appearance of the crystals it becomes clear, that at least those from

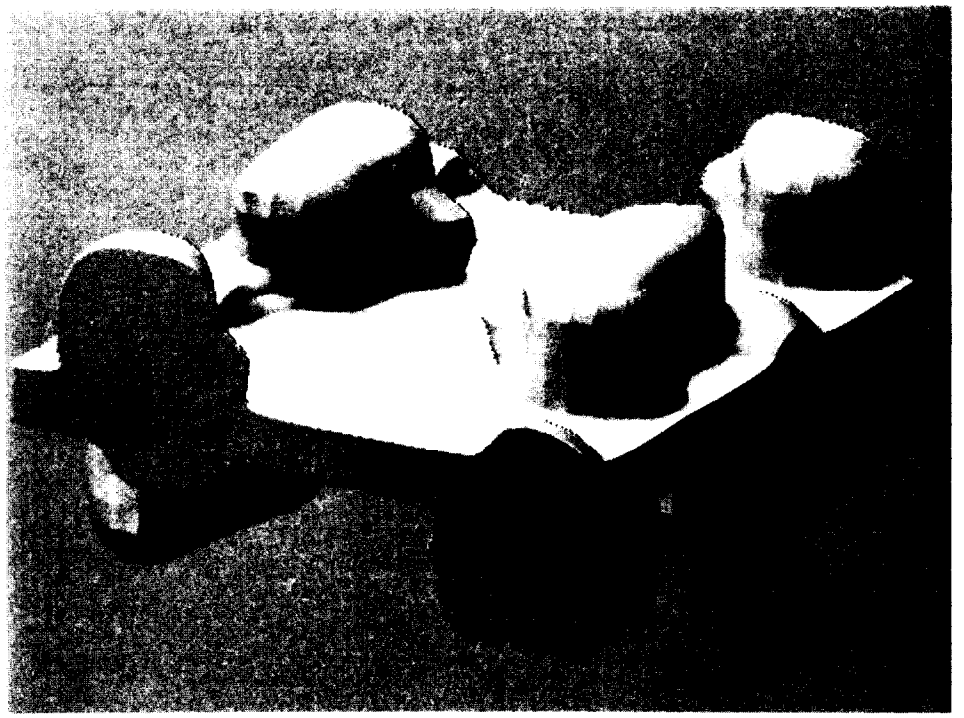

Fig. 10. Three-dimensional surface representation of fungal NADH dehydrogenase. The membrane is represented by a 4 nm thick sheet, out of which monomeric enzyme molecules protrude. These molecules are arranged alternating up–down across the membrane, with each molecule extremely asymmetrically located. Reproduced with permission from EMBL Research Reports 1986. Courtesy of Dr K. Leonard.

the beef heart enzyme allow some variation. It is unknown whether this represents a genuine structural difference. Furthermore, immunological similarities between both enzymes have as yet not been demonstrated.

The NADH dehydrogenase remains as yet the most complicated one. Important issues must be clarified; firstly, the necessity for a large number of polypeptides in the eukaryotic dehydrogenases as compared to the prokaryotic ones, as well as the precise number of constituent polypeptides. Secondly, the precise number of FeS clusters and the exact spatial organization of all prosthetic groups must be elucidated. A related issue is the function of possible EPR-silent FeS clusters; an issue that has been questioned by Kowal *et al.* (1986). They used magnetic circular dichroism (MCD) to assess the total number of FeS clusters in the soluble NADH dehydrogenase. The MCD data confirmed the EPR data in that four clusters were found. Therefore these authors rejected the existence of the EPR-silent clusters. Given the large variability of the Fe/FMN ratio, i.e. 16 to 23, both cluster arrangements of Kowal *et al.* (1986) and Ohnishi *et al.* (1985) account for the total amount of Fe present in each preparation. Given the relatively low purity levels of complex I, however, the proposed arrangement of four NADH-reducible FeS clusters arranged as one binuclear and three tetranuclear clusters seems to favour the *in vivo* situation. The matter, however, is still under dispute. Next, the overall structure needs to be elucidated at much higher resolution, either by means of electron microscopy in combination with sugar-embedding (Henderson *et al.*, 1986) or vitrification techniques (Rachel *et al.*, 1986) or by means of X-ray analysis of three-dimensional crystals (Deisenhofer *et al.*, 1985). The most important issues, however, are the underlying mechanisms of electron transport and of proton translocation. A

tentative scheme for redox-linked proton translocation has been presented by Ragan (1987). In this scheme proton translocation occurs in the FP fragment as a result of the redox reactions at the FMN, as well as in the hydrophobic residue as a result of redox reactions involving Q_{10}. In the cases of cytochrome reductase and cytochrome oxidase as yet only postulated schemes exist, despite the large amount of structural data on these two enzymes (Wikström and Saraste, 1984). Even for the F_0F_1 ATPase exotic models concerning ADP-phosphorylation exist (Mitchell, 1985). It thus appears that on the molecular level the link between protein structure and bioenergetics is far from clear.

Table 1. Subunit Composition of Bovine Mitochondrial F_0F_1 ATPase

Subunit	Mass	Copies
α	55164	3
β	51595	3
γ	30141	1
δ	15065	1
ϵ	5652	1
Inhibitor protein (IF1)	9578	1
Factor 6 (or F6, Fc2)	8000	?
OSCP	20967	2
a (ATPase 6)	24816	1
b	24700	2
c (DCCD binding protein or ATPase 9)	7602?	(6–10)
d	18603	1?
A6L	7965	1?
Factor B?		

IV. MITOCHONDRIAL F_0F_1-ATPASE

A. *Introduction*

The mitochondrial adenosinetriphosphatase (F_0F_1 ATPase, ATP synthase or complex V) catalyzes the last step in the synthesis of ATP in oxidative phosphorylation. It has three parts, usually depicted as F_0, F_1 and the stalk. F_0 is membrane-embedded and catalyzes the proton conduction across the membrane. F_1 is a water-soluble protein, connected by F_0 by a small stalk. F_1 contains the nucleotide and phosphate binding sites and catalyzes ATP synthesis, but synthesis is only carried out if F_1 is connected to F_0 by the stalk (the oligomycin sensitive F_0F_1 complex). The number of catalytic sites is still a matter of dispute, but most of the evidence is pointing to two catalytic and two non-catalytic sites out of the six nucleotide binding sites. Some of the many general reviews on mitochondrial and related ATP synthase complexes are found in Amzel and Pedersen (1983), Senior and Wise (1983) and Hoppe and Sebald (1984).

B. *Subunits of ATP Synthases*

Enzymes from different sources are very similar, but slight differences exist. Amongst the ATP synthases, the *E. coli* enzyme is the simplest defined so far, being a complex of eight different subunits (Foster and Fillingame, 1979). Five of them, α, β, γ, δ and ϵ, are located in the F_1 part. The α and β occur each in three copies. The remaining three subunits, a, b and c, constitute the F_0 part and the stalk. They are present in an unusual stoichiometry of 1:2:circa 10. The chloroplast enzyme has a similar composition, but has a fourth subunit in the F_0 part (Fromme *et al.*, 1987b).

Mitochondrial ATP synthase is somewhat more complex than the enzymes of *E. coli* and chloroplasts (Table 1). The F_1 part has the same five subunits (α–ϵ). The δ subunit of the mitochondrial enzyme, however, resembles the ϵ of the other systems, whereas the mitochondrial ϵ has no counterpart in the other ATP synthases. The ATP synthase inhibitor protein, which binds to subunit β, is a regulator protein whose primary function seems to be to prevent the hydrolysis of newly synthesized ATP (Ernster *et al.*, 1979).

The F_0 part consists of about five subunits (Walker *et al.*, 1987). Subunits a, b and c are related to the three *E. coli* subunits. Subunit d and the small hydrophobic subunit A6L (Fearnley and Walker, 1986) have no apparent bacterial homologues.

The composition of the stalk is not established but is presumed to comprise two water-soluble proteins designated coupling factor 6 (F6) and OSCP (oligomycin-sensitivity-conferring protein) (Hatefi, 1985a). The complete amino acid sequence of OSCP has been established (Ovchinnikov *et al.*,

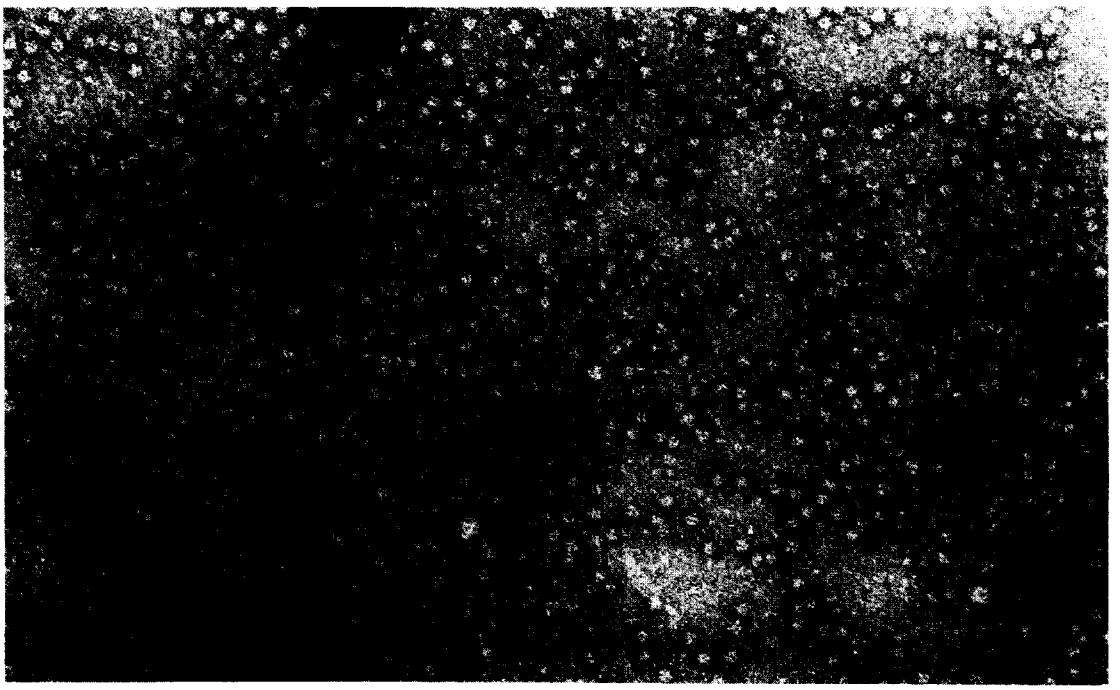

Fig. 11. Field showing single F_1 ATP synthase molecules used for image analysis. Estimated integrated object dose was 5500 electrons/nm^2. Scale marker represents 100 nm.

1984); the protein contains 190 amino acids and has a molecular mass of 20,967. The presence of the OSCP subunit is necessary to render the ATP synthase activity sensitive to oligomycin in the reconstituted F_0F_1 complex (Kagawa and Racker, 1966). The hydrophobic subunit b from F_0 is perhaps also involved in the stalk between F_0 and F_1 (Walker *et al.*, 1987).

ATP synthases from other preparations indicate that even more subunits could be present. For instance, factor B has been proposed to form part of F_0 (Sanadi *et al.*, 1984). Walker *et al.* (1987), however, were unable to detect factor B in their ATP synthase preparation.

C. *Structure of* F_1

Several electron microscopical studies concern the structure of F_1. Most information has come from analysis of the different projections of single, isolated particles, seen in negatively stained samples (Fig. 11). The dominant view is a hexagonal projection with six peripheral masses and a seventh mass located in the centre (Munoz *et al.*, 1968; Tiedge *et al.*, 1983; Akey *et al.*, 1983; Boekema *et al.*, 1986b). Under most staining conditions applied this is the projection mostly observed. However, other and more rare views are shown in Tsuprun *et al.* (1984), see Fig. 12. These views are very characteristic and important for an impression of the three-dimensional structure of F_1. First, they found a view in which only four masses are seen, the two central ones both being an overlap of two masses (Fig. 12b). From the presence of this projection we can draw the conclusion that the structure is a hexagonal antiprism of six (close-to) globular-shaped masses, which must be the large α and β subunits. Another view shows rectangular projections of molecules (Fig. 12c). A trigonal antiprism, seen from the side, can be turned in such a way that it has a rectangular appearance. The ratio between the axes is then 1.07. However, Tsuprun *et al.* (1984) found a ratio of 1.3 for these rectangular side views. We found a similar ratio for

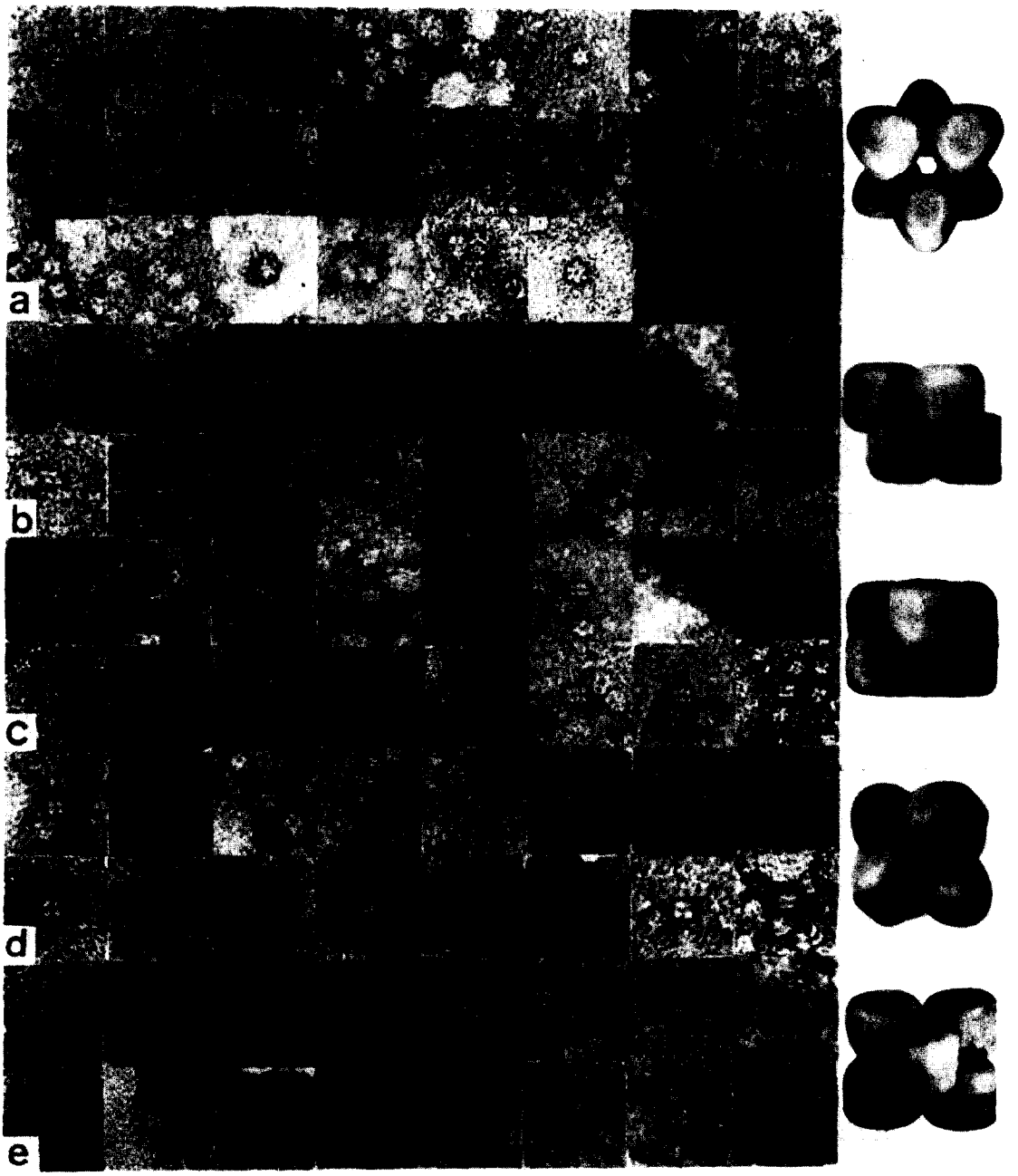

Fig. 12. Selected views of single F_1 ATP synthase molecules. Magnification is 300,000×. The views (A–E) correspond to the first five types of molecules visible. Reproduced with permission of Springer-Verlag. Courtesy of Dr V. L. Tsuprun.

such projections in electron micrographs of chloroplast ATP synthase (unpublished results); moreover, in bacterial F_1 ATP synthase the same rectangular side views exist (Biketov *et al.*, 1982). From this we must conclude that the hexagonal antiprism is slightly flattened.

A model showing a flattened hexagonal shape was also derived from tilt experiments of single F_1 particles (Tiedge *et al.*, 1983). These results, however, are less convincing, since preparation damage during the recording of the tilt series may also have contributed to the flattening. Recently, it was shown that the mass loss due to electron beam irradiation in a typical tilt series is of the order of 30% (Berriman and Leonard, 1986; Jésior and Wade, 1987).

Electron microscopy has also been carried out on small, three-dimensional F_1 crystals (Akey *et al.*, 1983). Electron micrographs of such crystals are in general difficult to interpret. Although the results are not very detailed, they do not contradict the model mentioned above. X-ray diffraction on crystals generally gives much higher resolution, and in combination with amino acid sequence data provides the insight into the protein structure. But until now, only a low resolution (1 nm) structure exists (Amzel *et al.*, 1982). Other groups, such as those of Walker in Cambridge, have also obtained three-dimensional crystals, and therefore, eventually within 5 to 10 years a detailed structure of F_1 could be available.

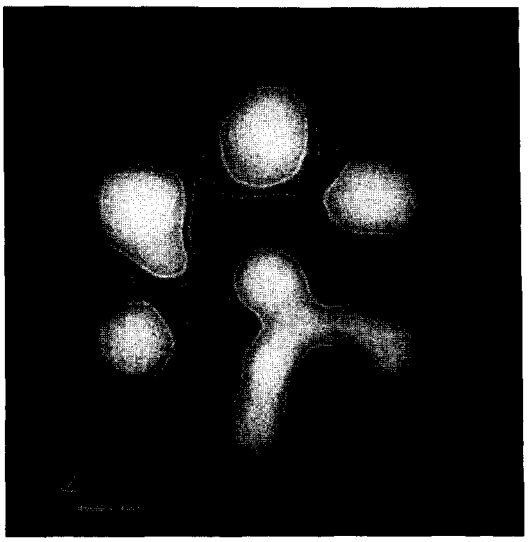

Fig. 13. Projected structure of F_1 ATP synthase after image analysis. The image results from a summation of 379 projections. Scale marker represents 2 nm. For details see Boekema *et al.* (1986b). Reproduced with permission from Elsevier Science Publishers B.V.

1. *Antibody labelling*

Since the masses of the α and β subunits differ only slightly (Table 1), it is not possible to discriminate between them in the images of the hexagonal projection. The arrangement of these subunits in the F_1 part has been deduced from immunoelectron microscopy (Lünsdorf *et al.*, 1984; Tiedge *et al.*, 1985). F_1 could be labelled with a maximum of three anti-α antibodies. The angle between two labelled α's was 120°, viz. the α and β subunits are alternating in projection. From this it is concluded that within the trigonal antiprism there must be a layer with three α's and a layer with three β's.

2. *Localization of the smaller subunits*

The presence of a seventh central mass in the hexagonal projection of F_1 molecules had already been observed many years ago (Munoz *et al.*, 1968). From the antibody work described above it became evident that this mass must comprise the three small subunits γ, δ and ϵ. Since only one copy of each subunit is present (Walker *et al.*, 1985) and since no repeating sequences within the amino acid backbone have been found for these subunits, the F_1 structure must be asymmetric. From the original noisy electron micrographs it is difficult to deduce the precise form and location of the seventh mass. Therefore image analysis was carried out on a large dataset of single F_1 molecules (Boekema *et al.*, 1986b). Molecular projections could be brought into equivalent orientations and averaged thereafter (Fig. 13). It was concluded that the seventh mass is located close to the centre, but slightly off its exact midpoint. It is V-shaped and its two legs point to two of the outer protein masses, most presumably being an α–β subunit pair. A similar result was obtained by Tsuprun *et al.* (1987). A ferritin label, which binds only to accessible SH groups on α, γ and ϵ, was used to localize these subunits. Up to four of the six external protein masses could be labelled and, therefore, one of the β subunits must form a complex with at least one of the small subunits, located partially on the molecule's external side.

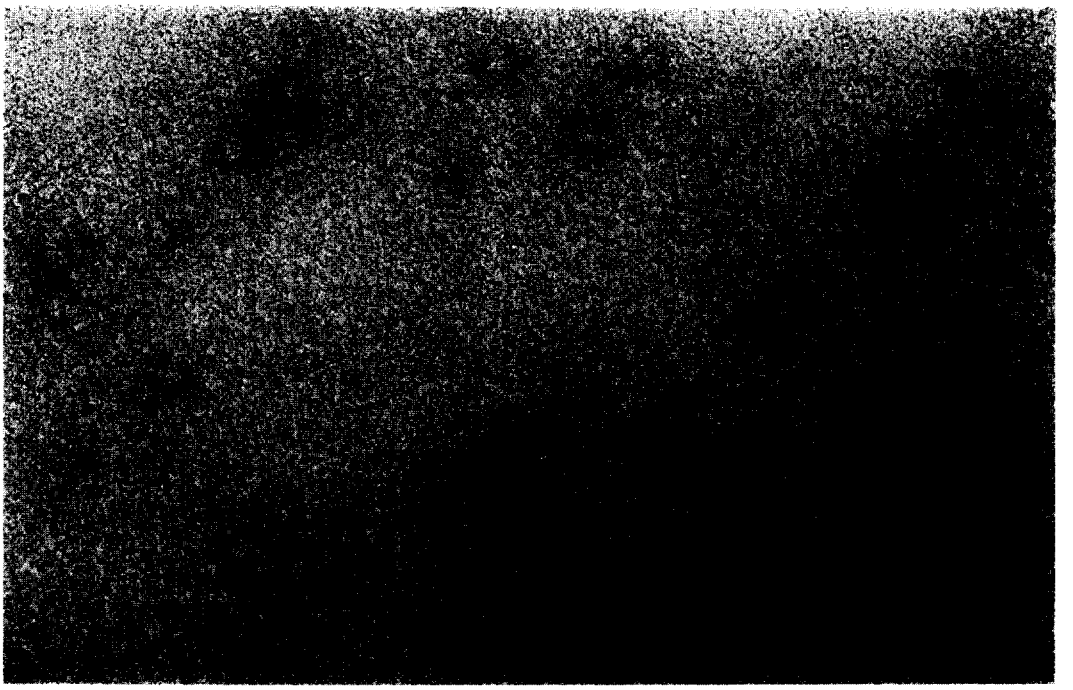

Fig. 14. Reconstituted F_0F_1 ATP synthase. F_0 and F_1 were reconstituted without the OSCP subunit. Arrows indicate the small gap between F_0 and F_1 parts. Scale marker represents 50 nm.

D. *Structure of the Stalk*

The dimensions of the stalk are most easily measured from isolated F_0F_1 ATPase molecules. We found that the dimensions of the stalk as seen in the projected complex are 4.3 × 4.3 nm. This is in agreement with results obtained by Tsuprun *et al.* (1987). The dimensions of the stalk, as seen in unstained, frozen-hydrated samples of *E. coli* ATP synthases, differ slightly, with only the diameter being significantly smaller (4.5 × 2.5 nm). This enzyme, however, is less complicated with only eight subunits instead of about 13 for the mitochondrial ATP synthase. Therefore a lesser number of subunits might be involved in the stalk.

OSCP is the main component of the stalk; but even in the absence of OSCP, isolated F_1 parts can combine with purified F_0 parts (MacLennan and Tzagoloff, 1968). If isolated F_0 and F_1 are mixed, the reconstituted complex shows a very small connection (about 1 nm) between both parts (Fig. 14). This suggests that besides the OSCP subunit other subunits also contribute to the stalk. Recently Walker *et al.* (1987) proposed that subunit b from the F_0 parts forms an important structural link between the F_0 and F_1 parts. This subunit could indeed be responsible for the connection as seen in Fig. 14, since most of its protein surface appears to be hydrophilic. Furthermore, F6 participates in the connection (Fessenden-Radan, 1972).

MacLennan and Asai showed already in 1968 that molecules from the isolated OSCP subunit have a strong tendency to arrange themselves into a multimeric aggregate. These aggregates have a diameter of about 10 nm and were interpreted as being tetramers. We observed very similar aggregates (Fig. 15). It seems, however, that in comparison to F_1 with a diameter of 11.5 nm and a mass of 371 kDa, these aggregates are remarkably large. Moreover, OSCP in the ATP synthase complex seems to be present in two copies (Penin *et al.*, 1985). Two OSCP molecules are likely to be arranged in the ATP synthase in the same way as

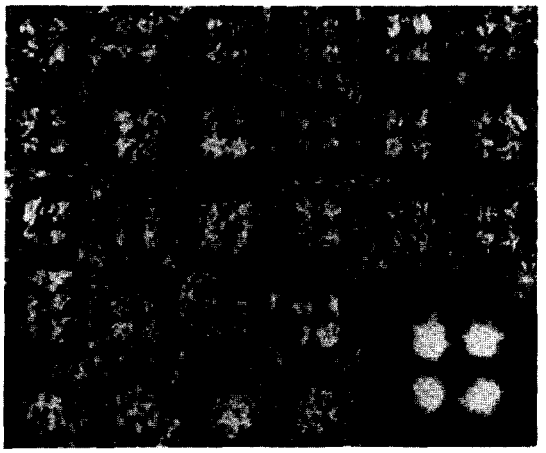

Fig. 15. Aggregates of isolated OSCP subunits. A gallery of 22 OSCP multimers, selected from digitized micrographs. Bottom row: four F_1 ATP synthase molecules on the same scale for comparison. Magnification is 530,000×. Bottom right: summation of 30 OSCP multimers after single-particle averaging.

in the aggregates of Fig. 14. However, if the aggregates are merely tetramers, as suggested by MacLennan and Asai (1968), two OSCP copies are difficult to fit within the dimensions of the stalk as measured before. Moreover, OSCP is an elongated protein with an axial ratio of >3 and with a hydrophobic central region (Dupuis *et al.*, 1983). From this it seems more likely that the OSCP multimers are octamers rather than tetramers.

E. *Structure of* F_0

Very little is known about the overall shape of the F_0 part. Single F_0F_1 particles, isolated from rat liver mitochondria with deoxycholate, have been presented by Soper *et al.* (1979). From these images it was concluded that the F_0 basepiece is about 12 nm long and 6 nm high. Since it is impossible that such F_0F_1 particles remain monodispersed without attached detergents, the real F_0 diameter is likely to be much smaller.

Isolated F_0F_1 molecules easily aggregate into smaller or longer strings (Fig. 16); the length of the strings depends on the detergent concentration. Similar aggregated molecules were also shown by Kagawa (1972) and Mullet *et al.* (1981). The diameter of F_0 in the membrane can be estimated from these string-like aggregated F_0F_1 ATPase molecules. Boekema *et al.* (1988) found a diameter of 6.4 nm. Using the same method, the diameter of chloroplast F_0 was found to be 6.2 nm. The height of F_0 is 8.9 nm.

On the basis of biochemical studies, two models have been proposed for the arrangement of the approximately 13 copies of the three *E. coli* F_0 ATP synthase subunits. In the model of Cox *et al.* (1986) one subunit a and two subunits b are placed within a ring of subunit c copies. In the model of Sebald *et al.* (1987) subunit a is situated on the periphery of the subunit c multimer. Recently, a multimeric complex of this subunit c was isolated from chloroplast ATP synthase (where it is called 'III') (Fromme *et al.*, 1987a). It has a diameter of 6.2 nm and a height of 6.4 nm and most likely contains 12 subunits. Interestingly, the diameter is similar to that of F_0, which could support the model of Cox for the chloroplast enzyme. It is, however, not known how much structural similarity mitochondrial F_0 has with the bacterial and chloroplast systems. Since the mitochondrial subunits a, b and c have sequence homologies with their counterparts of the other systems, at least some similarity can be expected. Mitochondrial subunit c also has the tendency to form aggregates (Kopecky *et al.*, 1986), but an aggregate similar to the one of chloroplasts has not yet been found.

F. *Orientation of* F_0 *and* F_1 *and arrangement of* F_0F_1 in situ

If we take the concept of the flattened trigonal antiprism as the overall structure of the F_1 part, then there are two principally different ways of the F_1 parts becoming attached to the F_0 parts. The first possibility is that the hexamer is arranged vertically to F_0. Tsuprun *et al.* (1987) found, by averaging over 20 projections, that F_1 is oriented with its hexagonal profile perpendicular to the membrane. The other possibility is that the hexagonal profile is parallel to the membrane (or F_0), as in a mushroom. Figure 15 taken from Boekema *et al.* (unpublished results) points to the latter possibility. A large number of F_1 parts in isolated F_0F_1 complexes are oriented with their smallest sides

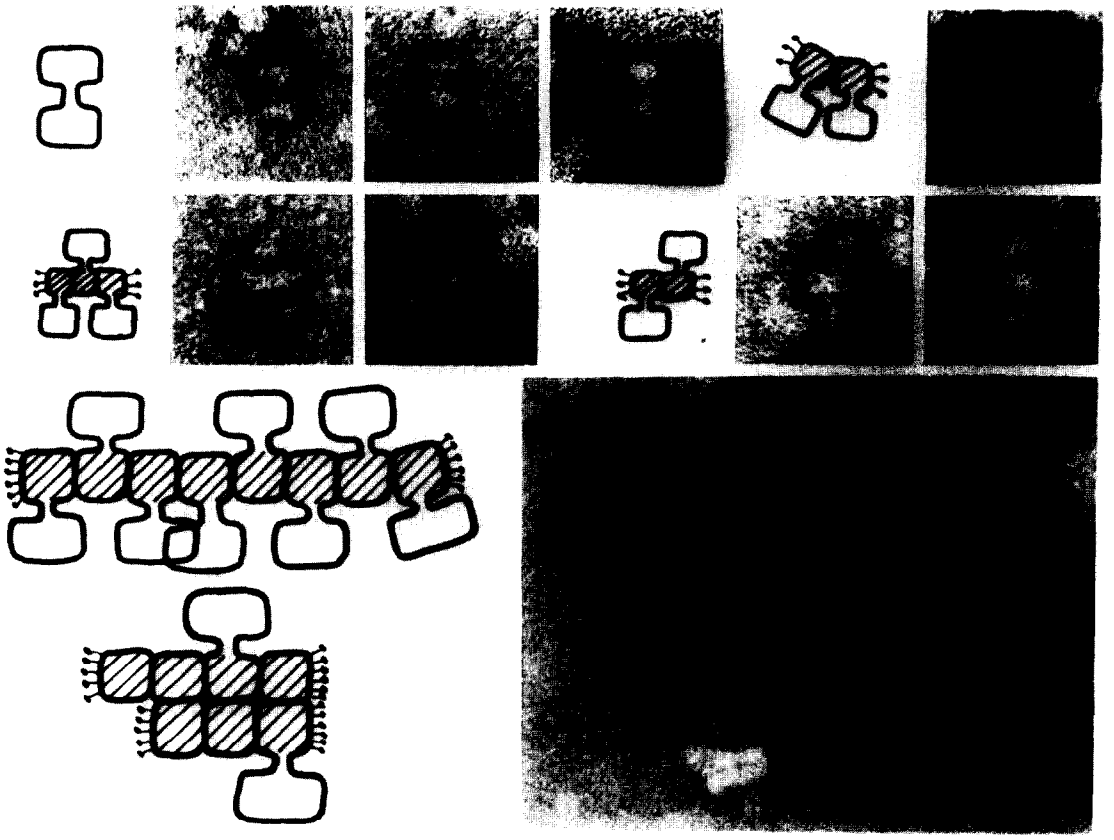

Fig. 16. Gallery of isolated F_0F_1 ATP synthases. Single complexes can be seen, as well as large aggregates. Schematic representations of aggregates indicate the different levels of aggregation. Scale marker represents 50 nm.

perpendicular to F_0. Since molecules in this side-view position are much more unstable on the carbon support film than molecules in the hexagonal projection, the finding that over 50% of the attached F_1 parts are in this position strongly points to the latter possibility.

Nevertheless, it is always possible that rearrangements take place. Moreover, conformational changes during the catalytic process occur. Although the tripartite ATP synthase is now widely accepted in the field of bioenergetics, the appearance of the F_0F_1 ATPase *in situ* has been in dispute for a long time. Some investigators propose that F_1 does not stick out from the membrane into the inner mitochondrial matrix, in a way that would be expected from negatively stained specimens (Sjöstrand, 1985). Wainio (1985) summarizes 40 papers, in which membranous ATP synthase was examined. In many cases no clear F_1 parts or stalks were seen, particularly if freeze–fracture methods were applied to study the inner mitochondrial membrane. However, recent results of Steinbrecht (1986) obtained with cryofixated and freeze-substituted mitochondria clearly show the F_1 knobs. Moreover, the appearance of a stalk is not an artifact of the negative staining technique, since Gogol *et al.* (1987) were able to demonstrate the stalk in unstained, frozen-hydrated specimens. In our opinion, the main reason for not always seeing the F_1 and the stalk in freeze–fracture studies could be the fact that other hydrophilic proteins are loosely associated with the mitochondrial inner membrane, shielding off the F_1 parts.

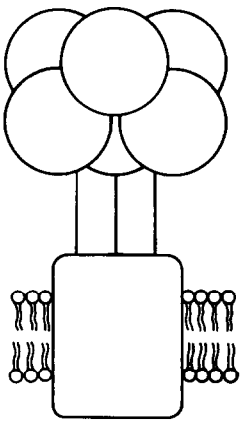

Fig. 17. Model of F_0F_1 ATP synthase. The model shows the enzyme incorporated in the membrane; lower three subunits of the F_1 part are most presumably the α subunits. For details see text.

V. SUMMARY AND CONCLUSIONS

The results of Section IV can be summarized in a simple ATP synthase model (Fig. 17). This model implies that either the α or the β subunits must be closer to the membrane. The work of Gao and Bauerlein (1987) indicates that the α subunits are closer to the membrane. Although the overall structure is more or less clear, important questions need to be clarified. First, the number and the arrangement of the subunits in the F_0 part must be known. Second, the exact shape of F_1, and particularly the shape of the large subunits needs to be elucidated. On the basis of fluorescence resonance energy transfer measurements by McCarty and Hammes (1987), a model was presented showing large oblong subunits. Such 'banana-shaped' subunits, which are also presented in the many phantasy models (e.g. Walker *et al.*, 1982), are very unlikely in view of the electron microscopical results, although the large subunits do not need to be exactly spherical. The third and most interesting central question is on the changes in the structure that take place during the different steps in the synthesis of ATP. It can now be taken as proven that the energy transmitted to the ATP synthase is used to induce a conformational change in the latter enzyme, in such a way as to bring about the energy-requiring dissociation of already synthesized ATP (Penefsky, 1985 and reviewed in Slater, 1987). But the way in which the three parts of the ATP synthase are involved is completely unknown. It is rather puzzling that such a long distance exists between the catalytic sites, which are on the interface of the α and β subunits and the F_0 part where the proton movements occur, which, according to Mitchell's theory (1961), is the driving force for the synthesis of ATP. Perhaps alternative mechanisms such as the collision hypothesis formulated by Herweijer *et al.* (1985) are more realistic in describing the mechanism of ATP synthesis. It would bring the complexes I and V close together, not only in the artificial way treated in this paper, but in a useful way for energy conversion.

Acknowledgements—E.J.B. wishes to thank Prof. Dr E. Zeitler for his continuous support of this work. We acknowledge the contribution of Drs S. P. J. Albracht and J. A. Berden to this work, both at the B.C.P. Jansen Institute, Department of Biochemistry, in Amsterdam. We are grateful to Drs Hatefi, Leonard and Tsuprun, who kindly gave permission to use their figures. We thank Mr K. Gilissen for printing the micrographs. These investigations have been supported by the Netherlands Organization for Chemical Research (SON) with financial aid from the Netherlands Organization for Scientific Research (NWO) and by the Deutsche Forschungsgemeinschaft (Sonderforschungsbereich 312).

REFERENCES

Akey, C. W., Spitsberg, V. and Edelstein, S. J., 1983. Electron microscopy of beef heart F_1-ATPase crystals. *J. biol. Chem.*, **258,** 3222–3229.

Albracht, S. P. J. and Bakker, P. T. A., 1986. Evidence for two independent pathways of electron transfer in mitochondrial NADH:Q oxidoreductase. II. Kinetics of reoxidation of the reduced enzyme. *Biochim. biophys. Acta*, **850,** 423–428.

Amos, L. A., Henderson, R. and Unwin, P. N. T., 1982. Three-dimensional structure determination by electron microscopy of two-dimensional crystals. *Prog. Biophys. molec. Biol.*, **39,** 183–231.

Amzel, L. M., McKinney, M., Narayan, P. and Pedersen, P. L., 1982. Structure of the mitochondrial F_1 ATPase at 9 Å resolution. *Proc. natn. Acad. Sci., U.S.A.*, **79,** 5852–5856.

Amzel, L. M. and Pedersen, P. L., 1983. Proton ATPases: structure and mechanism. *A. Rev. Biochem.*, **52,** 801–824.

Bakker, P. T. A. and Albracht, S. P. J., 1986. Evidence for two independent pathways of electron transfer in mitochondrial NADH:Q oxidoreductase. I. Pre-steady-state kinetics with NADPH. *Biochim. biophys. Acta*, **850,** 413–422.

Beinert, H. and Albracht, S. P. J., 1982. New insights, ideas and unanswered questions concerning iron–sulfur clusters in mitochondria. *Biochim. biophys. Acta*, **683,** 245–277.

Berriman, J. and Leonard, K., 1986. Methods for specimen

thickness determination in electron microscopy. *Ultramicroscopy*, **19,** 349–366.

Biggs, D. R., Hauber, J. and Singer, T. P., 1963. Studies on the respiratory chain-linked reduced nicotinamide adenine dinucleotide dehydrogenase. XII. Interrelations of NADH-cytochrome *c* reductase and NADH-Coenzyme Q reductase. *J. biol. Chem.*, **242,** 4563–4567.

Biketov, S. F., Kasho, V. N., Kozlov, I. A., Mileykovskaya, Y. I., Ostrovsky, D. N., Skulachev, V. P., Tikhonova, G. V. and Tsuprun, V. L., 1982. F_1-like ATPase from anaerobic bacterium *Lactobacillus casei* contains six similar subunits. *Eur. J. Biochem.*, **129,** 241–250.

Boekema, E. J. and Van Bruggen, E. F. J., 1983. Structure of bovine mitochondrial NADH:ubiquinone oxidoreductase studied by electron microscopy. In: *Structure and Function of Membrane Proteins*, Quagliariello, E. and Palmieri, F. (eds.), Elsevier, Amsterdam, 237–244.

Boekema, E. J., Van Breemen, J. F. L., Keegstra, W., Van Bruggen, E. F. J. and Albracht, S. P. J., 1982. Structure of NADH:Q oxidoreductase from bovine heart mitochondria studied by electron microscopy. *Biochim. biophys. Acta*, **679,** 7–11.

Boekema, E. J., Van Heel, M. G. and Van Bruggen, E. F. J., 1984. Three-dimensional structure of bovine NADH:ubiquinone oxidoreductase of the mitochondrial respiratory chain. *Biochim. biophys. Acta*, **787,** 19–26.

Boekema, E. J., Van Heel, M. G. and Van Bruggen, E. F. J., 1986a. Preparation of two-dimensional crystals of complex I and image analysis. *Meth. Enzym.*, **126,** 344–353.

Boekema, E. J., Berden, J. A. and Van Heel, M. G., 1986b. Structure of mitochondrial F_1-ATPase studied by electron microscopy and image processing. *Biochim. biophys. Acta*, **851,** 353–360.

Boekema, E. J., Schmidt, G., Gräber, P. and Berden, J. A., 1988. Structure of chloroplast and mitochondrial ATP-synthase studied by electron microscopy. *Z. Naturw.*, (in press).

Boyer, P. D., Chance, B., Ernster, L., Mitchell, P., Racker, E. and Slater, E. C., 1977. Oxidative phosphorylation and photophosphorylation. *A. Rev. Biochem.*, **46,** 955–1026.

Brink, J., Hovmöller, S., Ragan, C. I., Cleeter, M. W. J., Boekema, E. J. and Van Bruggen, E. F. J., 1987. The structure of NADH:ubiquinone oxidoreductase from beef-heart mitochondria. Crystals containing an octameric arrangement of iron–sulphur protein fragments. *Eur. J. Biochem.*, **166,** 287–294.

Chen, S. and Guillory, R. J., 1981. Studies on the interaction of arylazido-β-alanyl NAD^+ with the mitochondrial NADH dehydrogenase. *J. Biol. Chem.*, **256,** 8318–8323.

Chomyn, A., Mariottini, P., Cleeter, M. W. J., Ragan, C. I., Matsuno-Yagi, A., Hatefi, Y., Doolittle, R. F. and Attardi, G., 1985. Six unidentified reading frames of human mitochondrial DNA encode components of the respiratory-chain NADH dehydrogenase. *Nature*, **314,** 592–597.

Chomyn, A., Cleeter, M. W. J., Ragan, C. I., Riley, M., Doolittle, R. F. and Attardi, G., 1986. URF6, last unidentified reading frame of human mtDNA, codes for an NADH dehydrogenase subunit. *Science*, **234,** 614–618.

Cleeter, M. W. J. and Ragan, C. I., 1985. The polypeptide composition of the mitochondrial NADH:ubiquinone reductase complex from several mammalian species. *Biochem. J.*, **230,** 739–746.

Cleeter, M. W. J., Banister, S. H. and Ragan, C. I., 1985. Chemical cross-linking of mitochondrial NADH dehydrogenase from bovine heart. *Biochem. J.*, **227,** 467–474.

Costello, M. J. and Frey, T. G., 1987. Membrane proteins of the mitochondrion. In: *Electron Microscopy of Proteins, Vol. 6, Membranous Structures*, Harris, J. R. and Horne, R. W. (eds.), Academic Press, London, 378–443.

Cox, G. B., Fimmel, A. L., Gibson, F. and Hatch, L., 1986. The mechanism of ATP synthase: a reassignment of the functions of the b and a subunits. *Biochim. biophys. Acta*, **849,** 62–69.

Crane, F. L., Arntzen, C. J., Hall, J. D., Ruzicka, F. J. and Dilley, R. A., 1969. Binary membranes in mitochondria and chloroplasts. In: *Autonomy and Biogenesis of Mitochondria and Chloroplasts*, Boardman, N. K., Linnae, A. W. and Smillie, R. M. (eds.), North Holland, Amsterdam, London, 53–69.

Cremona, T., Kearney, E. B., Villavicencio, M. and Singer, T. P., 1963. Studies on the respiratory chain-linked DPNH dehydrogenase. V. Transformation of DPNH dehydrogenase to DPNH-cytochrome reductase and diaphorase under the influence of heat, proteolytic enzymes and urea. *Biochem. Z.*, **338,** 407–442.

Deatherage, J. F., Henderson, R. and Capaldi, R. A., 1982. Three-dimensional reconstruction of cytochrome *c* oxidase vesicles in negative stain. *J. molec. Biol.*, **158,** 487–499.

Deisenhofer, J., Epp, O., Miki, K., Huber, R. and Michel, H., 1985. Structure of the protein subunits in the photosynthetic reaction centre of *Rhodopseudomonas viridis* at 3Å resolution. *Nature*, **318,** 618–624.

Dooijewaard, G. and Slater, E. C., 1976a. Steady-state kinetics of high molecular weight (type-I) NADH dehydrogenase. *Biochim. biophys. Acta*, **440,** 1–15.

Dooijewaard, G. and Slater, E. C., 1976b. Steady-state kinetics of low molecular weight (type-II) NADH dehydrogenase. *Biochim. biophys. Acta*, **440,** 16–35.

Dooijewaard, G., De Bruin, G. J. M., Van Dijk, P. J. and Slater, E. C., 1984. Characterization of type-I NADH dehydrogenase. Polydispersity, molecular weight and polypeptide composition. *Biochim. biophys. Acta*, **501,** 458–469.

Dupuis, A., Zaccai, G. and Satre, M., 1983. Optical properties and small-angle neutron scattering of bovine heart mitochondrial oligomycin sensitivity conferring protein. *Biochemistry*, **22,** 5951–5956.

Earley, F. G. P. and Ragan, C. I., 1984. Photoaffinity labelling of mitochondrial NADH dehydrogenase with arylazido-amorphigenin, an analogue of rotenone. *Biochem. J.*, **224,** 525–534.

Ernster, L., Carlsson, C., Hundal, T. and Nordenbrand, K., 1979. Mitochondrial ATPase inhibitor: properties and applications. *Meth. Enzym.*, **55,** 399–407.

Fearnley, I. M. and Walker, J. E., 1986. Two overlapping genes in bovine mitochondrial DNA encode membrane components of ATP synthase. *EMBO J.*, **5,** 2003–2008.

Fessenden-Radan, J. M., 1972. Purification and properties of a new coupling factor required for oxidative phosphorylation in silico-tungstate-treated submitochondrial particles. *J. biol. Chem.*, **247,** 2351–2357.

Foster, D. L. and Fillingame, R. H., 1979. Energy-Transducing H^+-ATPase of *Escherichia coli*. Purification, reconstitution, and subunit composition. *J. biol. Chem.*, **254,** 8230–8236.

Frank, J., 1982. New methods for averaging non-periodic objects and distorted crystals in biological electron microscopy. *Optik*, **63,** 67–80.

Fromme, P., Boekema, E. J. and Gräber, P., 1987a. Isolation and characterization of a supramolecular complex of sub-

unit III of the ATP-synthase from chloroplasts. *Z. Naturf.*, **42C,** 1239–1245.

Fromme, P., Gräber, P. and Salnikow, J., 1987b. Isolation of a fourth subunit in the membrane part of the chloroplast ATP-synthase. *FEBS Lett.*, **218,** 27–30.

Gao, Z. and Bauerlein, E., 1987. Identifying subunits of ATP synthase TF_0. F_1 in contact with phospholipid head groups. *FEBS Lett.*, **223,** 366–370.

Gay, N. and Walker, J. E., 1985. Two genes encoding the bovine mitochondrial ATP synthase proteolipid specify precursors with different import sequences and are expressed in a tissue-specific manner. *EMBO J.*, **4,** 3519–3524.

Gogol, E. P., Lücken, U. and Capaldi, R. A., 1987. The stalk connecting the F_1 and F_0 domains of ATP synthase visualized by electron microscopy of unstained specimens. *FEBS Lett.*, **219,** 274–278.

Gondal, J. A. and Anderson, W. M., 1985. The molecular morphology of bovine heart mitochondrial NADH-ubiquinone reductase. Cross-linking with dithiobis(succinimidyl propionate). *J. biol. Chem.*, **260,** 5931–5935.

Hatefi, Y., 1985a. The mitochondrial electron transport and oxidative phosphorylation system. *A. Rev. Biochem.*, **54,** 1015–1069.

Hatefi, Y., 1985b. The enzymes and the enzyme complexes of the mitochondrial oxidative phosphorylation system. In: *The Enzymes of Biological Membranes*, Martonosi, A. N., (ed.), Vol. 4, 2nd ed., Plenum Press, New York, 1–70.

Hatefi, Y. and Stempel, K. E., 1969. Isolation and enzymatic properties of the mitochondrial reduced DPNH dehydrogenase. *J. biol. Chem.*, **244,** 2350–2357.

Hatefi, Y. and Stigall, D. L., 1976. Metal-containing flavoprotein dehydrogenases. In: *The Enzymes*, Boyer, P. D., Lardy, H. and Myrback, K. (eds.), Academic Press, New York, 175–222.

Hatefi, Y., Haavik, A. G. and Griffiths, D. E., 1962. Studies on the electron transfer system. XI. Preparation and properties of the mitochondrial DPNH-coenzyme Q reductase. *J. biol. Chem.*, **237,** 1676–1680.

Henderson, R., Baldwin, J. M., Downing, K. H., Lepault, J. and Zemlin, F., 1986. Structure of purple membrane from *Halobacterium halobium*: Recording, measurement and evaluation of electron micrographs at 3.5Å resolution. *Ultramicroscopy*, **19,** 147–178.

Heron, C., Smith, S. and Ragan, C. I., 1979. An analysis of the polypeptide composition of bovine heart mitochondrial NADH-ubiquinone oxidoreductase by two-dimensional polyacrylamide-gel electrophoresis. *Biochem. J.*, **181,** 435–443.

Herweijer, M. A., Berden, J. A. and Slater, E. C., 1985. Uncoupler-inhibitor titrations of ATP-driven reverse electron transfer in bovine submitochondrial particles provide evidence for direct interaction between ATPase and NADH:Q oxidoreductase. *Biochim. biophys. Acta*, **849,** 276–287.

Hoppe, J. and Sebald, W., 1984. The proton conducting F_0-part of bacterial ATP synthases. *Biochim. biophys. Acta*, **768,** 1–24.

Hovmöller, S., Slaughter, M., Berriman, J., Karlsson, B., Weiss, H. and Leonard, K., 1983. Structural studies of cytochrome reductase. Improved membrane crystals of the enzyme complex and crystallization of a subcomplex. *J. molec. Biol.*, **165,** 401–406.

Ise, W., Haiker, H. and Weiss, H., 1985. Mitochondrial translation of the subunits of the rotenone-sensitive NADH:ubiquinone reductase in *Neurospora crassa*. *EMBO J.*, **4,** 2075–2080.

Jésior, J.-C. and Wade, R. H., 1987. Electron-irradiation flattening of negatively stained 2D protein crystals. *Ultramicroscopy*, **21,** 313–320.

Kagawa, Y. and Racker, E., 1966. Properties of a factor conferring oligomycin sensitivity on mitochondrial adenosine triphosphatase. *J. biol. Chem.*, **241,** 2461–2466.

Kagawa, Y., 1972. Reconstitution of oxidative phosphorylation. *Biochim. biophys. Acta*, **265,** 297–338.

Kim, C. H., Radermacher, M., Kessel, M., Frank, J. and King, T. E., 1985. Three-dimensional reconstruction of cytochrome oxidase vesicle crystals prepared by cholate solubilization. *J. Inorg. Biochem.*, **23,** 163–169.

Kopecky, J., Houstek, J., Szarska, E. and Drahote, Z., 1986. Electrophoretic behaviour of the H^+-ATPase proteolipid from bovine heart mitochondria. *J. Bioenerg. Biomembr.*, **18,** 507–519.

Kowal, A. T., Morningstar, J. E., Johnson, M. K., Ramsay, R. R. and Singer, T. P., 1986. Spectroscopic characterization of the number and type of iron–sulfur clusters in NADH:ubiquinone oxidoreductase. *J. biol. Chem.*, **261,** 9239–9245.

Lane, M. D., Pedersen, P. L. and Mildvan, A. S., 1986. The mitochondrion updated. *Science*, **234,** 526–527.

Lehninger, A. L., 1964. In: *The Mitochondrion*, Benjamin, W. A., New York.

Leonard, K., Wingfield, P., Arad, T. and Weiss, H., 1981. Three-dimensional structure of ubiquinol:cytochrome *c* reductase from *Neurospora crassa* mitochondria determined by electron microscopy of membrane crystals. *J. molec. Biol.*, **149,** 259–274.

Leonard, K., Haiker, H. and Weiss, H., 1987. Three-dimensional structure of NADH:ubiquinone reductase (Complex I) from *Neurospora crassa* determined by electron microscopy of membrane crystals. *J. molec. Biol.*, **194,** 277–286.

Liang, A. M. and Fisher, R. J., 1983. Subunit interaction in the mitochondrial H^+-translocating ATPase. *J. biol. Chem.*, **258,** 4784–4787.

Lünsdorf, H., Ehrig, K., Friedl, P. and Salton, M. R. J., 1984. Use of monoclonal antibodies in immuno-electron microscopy for the determination of subunit stoichiometry in oligomeric enzymes. *J. molec. Biol.*, **173,** 131–136.

MacLennan, D. M. and Asai, J., 1968. Studies on the mitochondrial adenosine triphosphatase system. V. Localization of the oligomycin-sensitivity conferring protein. *Biochem. biophys. Res. Commun.*, **33,** 441 447.

MacLennan, D. M. and Tzagoloff, A., 1968. Studies on the mitochondrial adenosine triphosphatase system. IV. Purification and characterization of the oligomycin-sensitivity conferring protein. *Biochemistry*, **7,** 1603–1610.

Mannella, C. A., 1982. Structure of the outer mitochondrial membrane: ordered arrays of porelike subunits in outer-membrane fractions from *Neurospora crassa* mitochondria. *J. Cell Biol.*, **94,** 680–687.

Matthews, B. W., 1968. Solvent content of protein crystals. *J. molec. Biol.*, **33,** 491–497.

McCarty, R. E. and Hammes, G. C., 1987. Molecular architecture of chloroplast coupling factor 1. *Trends Biochem. Sci.*, **12,** 234–237.

Michel, H., 1983. Crystallization of membrane proteins. *Trends Biochem. Sci.*, **8,** 56–59.

Mitchell, P., 1961. Coupling of phosphorylation to electron and hydrogen transfer by a chemiosmotic type of mechanism. *Nature*, **191,** 105–109.

Mitchell, P., 1985. Molecular mechanics of protonmotive F_0F_1 ATPases. Rolling well and turnstile hypothesis. *FEBS Lett.*, **182,** 1–7.

Mullet, J. E., Pick, U. and Arntzen, C. J., 1981. Structural analysis of the isolated chloroplast coupling factor and the *N,N'*-dicyclohexylcarboiimide binding proteolipid. *Biochim. biophys. Acta*, **642,** 149–157.

Munoz, E., Freer, J. H., Ellar, D. J. and Salton, M. R. J., 1968. Membrane-associated ATPase activity from *Micrococcus lysodeikticus*. *Biochim. biophys. Acta*, **150,** 531–533.

Ohnishi, T., 1979. Mitochondrial iron–sulfur flavodehydrogenases. In: *Membrane Proteins in Energy Transduction*, Capaldi, R. A. (ed.), Dekker, New York, 1–87.

Ohnishi, T. and Salerno, J. C., 1982. Iron–sulfur clusters in the mitochondrial electron-transport chain. In: *Iron–Sulfur Proteins, Vol. 4*, Spiro, T. G. (ed.), Wiley, New York, 285–327.

Ohnishi, T., Ragan, C. I. and Hatefi, Y., 1985. EPR studies of iron–sulfur clusters in isolated subunits and subfractions of NADH-ubiquinone oxidoreductase. *J. biol. Chem.*, **260,** 2782–2788.

Ovchinnikov, Yu. A., Modyanov, N. N., Grinkevich, V. A., Aldanova, N. A., Trubetskaya, O. E., Nazimov, I. V., Hundal, T. and Ernster, L., 1984. Amino acid sequence of the oligomycin sensitivity conferring protein (OSCP) of beef-heart mitochondria and its homology with the δ subunit of the F_1 ATPase of *Escherichia coli*. *FEBS Lett.*, **166,** 19–22.

Paech, C., Reynolds, J. G., Singer, T. P. and Holm, R. H., 1981. Structural identification of iron–sulfur clusters of the respiratory chain-linked NADH dehydrogenase. *J. biol. Chem.*, **256,** 3167–3170.

Penefsky, H. S., 1985. Mechanism of inhibition of mitochondrial adenosine triphosphatase by dicyclohexylcarboiimide and oligomycin: relationship to ATP synthesis. *Proc. natn. Acad. Sci., U.S.A.*, **82,** 1589–1593.

Penin, F., Archinard, P., Moradi-Ameli, M. and Godinot, C., 1985. Stoichiometry of the oligomycin-sensitivity-conferring protein (OSCP) in the mitochondrial F_0F_1-ATPase determined by an immunoelectrotransfer blot technique. *Biochim. biophys. Acta*, **810,** 346–353.

Ragan, C. I., 1976a. NADH-ubiquinone oxidoreductase. *Biochim. biophys. Acta*, **456,** 249–290.

Ragan, C. I., 1976b. The structure and subunit composition of the particulate NADH-ubiquinone reductase of bovine heart mitochondria. *Biochem. J.*, **154,** 295–305.

Ragan, C. I., 1980. The molecular organization of NADH dehydrogenase. In: *Subcellular Biochemistry, Vol. 7*, Roodyn, D. B. (ed.), Plenum Press, New York, 267–307.

Ragan, C. I., 1987. Structure of NADH-ubiquinone reductase (Complex I). *Curr. Topics Bioenerg.*, **15,** 1–36.

Ragan, C. I. and Cottingham, I. R., 1985. The kinetics of quinone pools in electron transport. *Biochim. biophys. Acta*, **811,** 13–31.

Ragan, C. I. and Hatefi, Y., 1986. Isolation of the iron–sulfur-containing polypeptides of NADH:ubiquinone oxidoreductase. *Meth. Enzym.*, **126,** 360–369.

Ragan, C. I. and Heron, C., 1978. The interaction between mitochondrial NADH-ubiquinone oxidoreductase and ubiquinol-cytochrome *c* oxidoreductase. Evidence for stoichiometric association. *Biochem. J.*, **174,** 783–790.

Ragan, C.I. and Racker, E., 1973. Resolution and reconstitution of the mitochondrial electron transport system. IV. The reconstitution of rotenone-sensitive reduced nicotinamide adenine dinucleotide-ubiquinone reductase from reduced nicotinamide adenine dinucleotide dehydrogenase and phospholipids. *J. biol. Chem.*, **248,** 6876–6884.

Ragan, C. I., Galante, Y. M., Hatefi, Y. and Ohnishi, T., 1982a. Resolution of mitochondrial NADH dehydrogenase and isolation of two iron-sulfur proteins. *Biochemistry*, **21,** 590–594.

Ragan, C. I., Galante, Y. M. and Hatefi, Y., 1982b. Purification of three iron–sulfur proteins from the iron–protein fragment of mitochondrial NADH-ubiquinone oxidoreductase. *Biochemistry*, **21,** 2518–2524.

Rachel, R., Jakubowski, U., Tietz, H., Hegerl, R. and Baumeister, W., 1987. Projected structure of the surface protein of *Deinococcus radiodurans* determined at 0.8 nm resolution by cryomicroscopy. *Ultramicroscopy*, **20,** 305–316.

Rieske, J. S., 1976. Composition, structure, and function of complex III of the respiratory chain. *Biochim. biophys. Acta*, **456,** 195–247.

Rossi, C., Cremona, T., Machinist, J. M. and Singer, T. P., 1965. Studies on the respiratory chain-linked NADH dehydrogenase. VIII. Inactivation, fragmentation, and protection by substrates. *J. biol. Chem.*, **240,** 2634–2643.

Sanadi, D. R., Pringle, M., Kantham, L., Hughes, J. B. and Srivastava, A., 1984. Evidence for the involvement of coupling factor B in the H^+-channel of the mitochondrial H^+-ATPase. *Proc. natn. Acad. Sci., U.S.A.*, **81,** 1371–1374.

Saxton, W. O. and Baumeister, W., 1982. The correlation averaging of a regularly arranged bacterial cell envelope protein. *J. Microscopy*, **127,** 127–138.

Schneider, H., Lemasters, J. J., Höchli, M. and Hackenbrock, C. R., 1980. Liposome–mitochondrial inner membrane fusion. *J. biol. Chem.*, **255,** 3748–3756.

Sebald, W. and Hoppe, J., 1981. On the structure and genetics of the proteolipid subunit of the ATP synthase complex. *Curr. Topics Bioenerg.*, **12,** 1–64.

Sebald, W., Weber, H. and Hoppe, J., 1987. Conformational stability of the proteolipid oligomer of the H^+-conducting F_0 of the ATP synthase. In: *Bioenergetics: Structure and Function of Energy Transducing Systems*, Ozawa, T. and Papa, S. (eds.), Springer, Berlin.

Senior, A. E. and Wise, J. G., 1983. The proton-ATPase of bacteria and mitochondria. *J. Membr. Biol.*, **73,** 105–124.

Sjöstrand, F. S., 1983. The diversity of function and structure of cellular membranes. In: *Subcellular Biochemistry, Vol. 9*, Roodyn, D. B. (ed.), Plenum Press, New York, 335–389.

Slater, E. C., 1983. The Q cycle, an ubiquitous mechanism of electron transfer. *Trends Biochem. Sci.*, **8,** 239–242.

Slater, E. C., 1987. The mechanism of the conservation of energy of biological oxidations. *Eur. J. Biochem.*, **166,** 489–504.

Soper, J. W., Decker, G. L. and Pedersen, P. L., 1979. Mitochondrial ATPase complex. A dispersed, cytochrome-deficient, oligomycin-sensitive preparation from rat liver. *J. biol. Chem.*, **254,** 11170–11176.

Steinbrecht, R. A., 1986. ATPase particles on mitochondrial cristae and the plasma membrane of an insect as demonstrated by freeze substitution. *Naturwissenschaften*, **73,** 275–276.

Tiedge, H., Schäfer, G. and Mayer, F., 1983. An electron microscopic approach to the quaternary structure of mitochondrial F_1-ATPase. *Eur. J. Biochem.*, **132,** 37–45.

Tiedge, H., Lünsdorf, H., Schäfer, G. and Schairer, H. U., 1985. Subunit stoichiometry and juxtaposition of the photosynthetic coupling factor 1: immunoelectron microscopy using monoclonal antibodies. *Proc. natn. Acad. Sci., U.S.A.*, **82,** 7874–7878.

Tsuprun, V. L., Mesyanzhinova, I. V., Kozlov, I. A. and Orlova, E. V., 1984. Electron microscopy of beef heart mitochondrial F_1-ATPase. *FEBS Lett.*, **167,** 285–290.

Tsuprun, V. L., Mesyanzhinova, I. V., Milgrom, Y. M. and Kalashnikova, T. Yu., 1987. Electron-microscopic studies on location of SH-groups in mitochondrial F_1-ATPase using a ferritin label. *Biochim. biophys. Acta*, **892,** 130–137.

Tzagoloff, A., 1982. In: *Mitochondria*, Plenum Press, New York and London.

Tzagoloff, A. and Myers, A. M., 1986. Genetics of mitochondrial biogenesis. *A. Rev. Biochem.*, **55,** 249–285.

Wainio, W. W., 1985. Are there knobs on energy transducing membranes *in situ? J. Ultrastr. Res.*, **93,** 138–143.

Walker, J. E., Saraste, M. and Gay, N. J., 1982. *E. coli* F_1-ATPase interacts with a membrane protein component of a proton channel. *Nature*, **298,** 867–869.

Walker, J. E., Fearnley, I. M., Gay, N. J., Gibson, B. W., Northrop, F. D., Powell, S. J., Runswick, M. J., Saraste, M. and Tybulewicz, V. L. J., 1985. Primary structure and subunit stoichiometry of F_1-ATPase from bovine mitochondria. *J. molec. Biol.*, **184,** 677–701.

Walker, J. E., Runswick, M. J. and Poulter, L., 1987. ATP synthase from bovine mitochondria. The characterization and sequence analysis of two membrane-associated subunits and of the corresponding cDNAs. *J. molec. Biol.*, **197,** 98–100.

Watari, H., Kearney, E. B. and Singer, T. P., 1963. Studies on the respiratory chain-linked NADH dehydrogenase. IV. Transformation of the dehydrogenase into cytochrome *c* reductase-diaphorase by the action of acid-ethanol. *J. biol. Chem.*, **238,** 4063–4073.

Wikström, M. and Saraste, M., 1984. The mitochondrial respiratory chain. In: *Bioenergetics, Vol. 9*, Ernster, L. (ed.), Elsevier Science Publishers B. V., Amsterdam, New York and Oxford, 49–94.